Eur. Phys. J. B (2014) 87: 115
DOI: 10.1140/epjb/e2014-41063-0

THE EUROPEAN PHYSICAL JOURNAL B

Regular Article

Stationary Josephson current in junctions involving d-wave superconductors with charge density waves: the temperature dependence and deviations from the law of corresponding states

Alexander M. Gabovich[1], Mai Suan Li[2], Henryk Szymczak[2], and Alexander I. Voitenko[1,a]

[1] Institute of Physics, NASU, 46, Nauka Ave., 03680 Kyiv, Ukraine
[2] Institute of Physics, PAN, Al. Lotników 32/46, 02-668 Warsaw, Poland

Received 8 December 2013
Published online 19 May 2014 –

Abstract. Stationary Josephson current I_c in symmetric and non-symmetric junctions involving d-wave superconductors with charge density waves (CDWs) was calculated. It was found that, if CDWs are weak or absent, there exists an approximate proportionality between I_c and the product of superconducting order parameters in the electrodes (the law of corresponding states) for several factors affecting those quantities, such as the temperature, T, or one of the parameters characterizing the combined CDW superconducting phase (the degree of the Fermi surface dielectric gapping and the ratio between the parent superconducting and CDW order parameters). Otherwise, the dependences $I_c(T)$ were shown to deviate from those in the absence of CDWs, and the relevant corresponding-state dependences from linearity, the deviations being especially strong at certain rotation angles of crystalline electodes with respect to the junction plane. Hence, making use of specially designed experimental setups and analyzing the $I_c(T)$ and corresponding-state dependences, the existence of CDWs in cuprates and other non-conventional superconductors can be detected.

1 Introduction

The temperature, T, dependence of the stationary Josephson critical current, I_c, between two isotropic Bardeen-Cooper-Schrieffer (BCS) superconductors considered in the weak-coupling approximation [1] was first obtained by Ambegaokar and Baratoff [2,3] in the tunnel Hamiltonian approach [4–6]. The original derivation assumed no tunnel directionality and neglected any possible energy and momentum dependences of the tunnel Hamiltonian matrix elements $\widetilde{T}_{\mathbf{pq}}$. Those results were soon generalized to anisotropic Fermi surfaces (FSs) and anisotropic superconducting gaps [7,8]. Later on, after the spin-fluctuation-driven $d_{x^2-y^2}$-wave superconductivity scenario was proposed for high-T_c oxides [9–11], the dependences $I_c(T)$ were numerically calculated for the d-wave case as well [12,13]. It is important that in the case of anisotropic pairing interaction leading to d-wave symmetry of the superconducting order parameter one should take into account the momentum dependences of $\widetilde{T}_{\mathbf{pq}}$ in order to avoid the trivial vanishing of the overall current I_c due to the mutual compensation of positive- and negative-lobe contributions [14,15].

Since the calculations of I_c for tunneling between s-wave superconductors can be (and usually are) restricted to the non-directional case [2,3,16,17], the normalized (to the zero-temperature value) behavior of $I_c(T)$ is determined solely by the input dependences of the superconducting energy gaps $\Delta(T)$ and $\Delta'(T)$ characterizing the left- and right-hand-side electrodes, respectively, because other properties of junction barrier can be factorized into the normal-state junction resistance R_N. At the same time, the normalized gap function $\Delta(T)$ of a weak-coupling isotropic BCS superconductor is described by the universal Mühlschlegel function [18]. Namely, the dependence $\delta = \Delta/\Delta_0$ versus $t = T/\Delta_0$ is a function $s\text{Mü}(t)$, with the characteristic ratio between the normalized zero-temperature gap $\delta(0) = \Delta(T = 0)/\Delta_0$ (in the selected normalization, $\delta(0) = 1$) and the critical temperature $t_c = T_c/\Delta_0$ being equal to about 1.76 (the Boltzmann constant $k_B = 1$, $\Delta_0 = \Delta(T = 0)$). As stems from, e.g., (19) in reference [19], in the case of d-wave pairing, the gap on every small section of the Fermi surface (FS) also "tries" to follow the Mühlschlegel equation, but the cosine angular behavior over the FS imposed by the pairing anisotropy [20,21] slightly modifies the $\delta(t)$ dependence into the $d\text{Mü}(t)$ one and brings about the characteristic ratio $\delta(0)/t_c \approx 2.14$. In other words, for every pairing mechanism, we obtain a single relevant characteristic value independent of specific superconducting parameters, the situation being analogous to the theory of ideal gas where all problem parameters are combined to produce

[a] e-mail: voitenko@iop.kiev.ua

the gas constant R. The functions sMü(t) and dMü(t) can also be regarded as laws of corresponding states [22,23], in analogy, e.g., with the reduced van der Waals equation in the theory of gases and liquids [24]. This circumstance leads in the case of the isotropic pairing to the universality of the curve $I_c(T)/I_c(0)$ versus T/T_c for symmetric junctions, as well as to the universal character of $I_c(T)$ as a functional of $\Delta(T)$. It is remarkable that the T-behavior of the isotropic BCS Δ almost coincides numerically [25] with a much simpler dependence of the magnetization in the molecular-field Curie-Weiss model for ferromagnetism [26]. The formal similarity between the order parameters takes place, despite that the free energies in both models differ substantially [25,27].

It would be instructive to find a similar universality and check its possible violations for $I_c(T)$ in the case of d-wave superconductors [28,29], where an account of tunnel directionality [30,31] is unavoidable and complicates the issue [14,15]. In this work, we tried to show that since the superconducting gap is the crucial factor driving the current behavior the relation between current and superconducting gap magnitudes is rather robust and can be regarded as the approximately valid law of corresponding states. However, the aim of this paper is more general. Namely, we intend to elucidate the influence of combined structural and charge modulations inherent to high-T_c oxides on the stationary Josephson current.

Indeed, it is known that the so-called pseudogaps coexist and compete with superconductivity in cuprates [19,32–47], being, in our opinion, a consequence of the inherent charge density waves (CDWs) and concomitant periodic lattice distortions [19,32–36,38,39,42,44,48–55]. One should bear in mind that the powerful conventional X-ray or neutron scattering technique may fail in detecting CDW reflexes due to the smallness of structural distortions, a patch-like character of CDW domains, or a possible fluctuating nature of CDWs. This was proved true when, contrary to the previous results [56] CDWs were found in the CuO_2 planes of $YBa_2Cu_3O_{6+x}$ [57] and $(Y,Nd)Ba_2Cu_3O_{6+x}$ [48] using the resonance X-ray scattering method. The same method made it possible to compare CDW modulations for $[(Y,Nd)Ba_2Cu_3O_{6+x}]$ and $[La_{2-x-y}(Sr,Ba)_x(Eu,Nd)_yCuO_4]$ oxide families [58]. It turned out that CDW states have large correlation lengths of 259 ± 9 Å for $La_{1.875}Ba_{0.125}CuO_4$ and 55 ± 15 Å for $YBa_2Cu_3O_{6.6}$, so that CDWs can be regarded as static rather than fluctuating ones. At the same time, charge modulations fluctuate at higher temperatures [48], as it should be in systems with a reduced dimensionality [59,60].

We emphasize that CDWs manifest themselves in all hole-doped cuprates, even in the tetragonal $HgBa_2CuO_{4+\delta}$ [61]. Therefore, they most probably originate from charge carriers in the square CuO_2 plane, as is usually assumed in theoretical considerations including ours (see below).

If the d-wave Cooper pairing is assumed to dominate in those materials (the majority of experimental data supports this viewpoint [62,63], although the isotropic or extended s-wave contribution to the superconducting order parameter cannot be excluded from consideration [64–66]), the interplay between CDWs and superconductivity can lead to a lot of interesting peculiarities, in particular, in quasiparticle and coherent tunneling [19,41,66–71]. Therefore, one may expect that CDWs would reveal themselves as factors that (i) distort the Ambegaokar and Baratoff dependence $I_c(T)$ [2,3], and (ii) violate the law of corresponding states (if any) between the T-dependences of I_c and Δ. It is important that CDW superconductors allow one to vary their superconducting gaps by changing not only the temperature but also other parameters associated with the dielectric (in addition to the superconducting) gapping of their FS and, hence, affect the magnitude of the stationary Josephson current. The same is expected to be true for the related extended s-wave symmetry with a similar angular dependence of the superconducting order parameter. The relevant calculations are carried out in this work for different rotations of CDW superconducting electrodes with respect to the junction plane. A comparison with the Josephson current between partially dielectrized CDW isotropic s-wave superconductors is made. Various properties of the latter model have been studied earlier [72–88].

Here, we continue to study tunneling through junctions with partially gapped d-wave CDW superconductors. The dependences of the stationary Josephson current I_c on the electrode orientation with respect to the junction plane have been studied in detail previously [66]. This paper is devoted to the analysis of not less important I_c dependences on the intrinsic parameters of materials concerned, as well as on the temperature. Meanwhile, in the course of research, we found that the electrode orientation affects the indicated dependences. Therefore, the problem will be analyzed making allowance for single-crystal-electrode rotations. It should be noted that the results presented here can be applied not only to high-T_c oxides but also to other quasi-two-dimensional superconductors with anisotropic Cooper pairing and CDWs.

It should be noted that our calculations are made for the case of low barrier transparency, i.e. when the insulating interlayer in the junctions is wide enough and the tunneling-Hamiltonian approach is valid [89,90].

2 Formulation

Following evidence discussed in our previous publications [41,66,68–71] and references therein, we consider a CDW superconductor (CDWS) with a two-dimensional FS. The superconducting d-wave gap spans the whole FS, whereas the dielectric mean-field CDW gap develops on the nested (dielectrized, d) sections only. The CDW-vectors $\mathbf{Q}$'s connect those FS sections. The non-nested sections remain non-dielectrized (nd). The orientations of $\mathbf{Q}$'s are determined by the crystal lattice, i.e. they are directed along the $\mathbf{k}_x$- and $\mathbf{k}_y$-axes in the momentum space (antinodal nesting) [19,91,92]. The interplay between antinodal and nodal nesting (revealed, in particular, in spin

excitations of La-based cuprates [93,94]) was discussed recently [95]. Modulations caused by the nodal nesting do not manifest themselves in tunneling phenomena and hence are left beyond the scope of this work.

It should be noted that, in agreement with the X-ray data that revealed large CDW-order-parameter coherence lengths [58], we do not examine an interesting possibility of fluctuating CDWs [96–98] instead of the static ones. Hence, we neglect superconducting fluctuations, sometimes claimed to extend far above T_c [48,99]. One more remark should be made concerning the fluctuating aspect of CDW manifestations in cuprates. Nuclear magnetic resonance (NMR) studies of CDWs in the vortex cores of $YBa_2Cu_3O_{6+\delta}$ demonstrated [54] that CDWs are *static inside the cores*, whereas they are weakened in the absence of the magnetic field and claimed to have a fluctuating nature. (Static CDWs with a local "nematic" C_2 symmetry inside the vortex cores were found also for $Bi_2Sr_2CaCu_2O_x$ [100].). According to our theory, this fact may mean that superconductivity strongly suppresses CDWs for the investigated doping levels. Hence, CDWs are on the verge of T-dependent disappearance (reentrance) [19,35,36,41,67]. Such a situation is not mandatory, being severely dependent on the system parameters. That is why CDWs are quite robust in the general case, even within the superconducting dome.

In high-T_c oxides, CDWs demonstrate four-fold ($N = 4$, the checkerboard configuration) or two-fold ($N = 2$, the unidirectional configuration, probably associated with an electronic nematic or smectic ordering [101,102]) symmetries [19,35,36,42,44,47,66] . The direction of either of two CDW vectors (for $N = 4$) or of the single one (for $N = 2$) is chosen as a reference one in the crystal. We select it to coincide with the basis vector $\mathbf{k}_x$. The magnitude of the CDW order parameter is assumed to be constant within the FS d-sections, each of the width 2α. Their position on the FS is described by the angular factor $f_\Sigma(\theta) = 1$ for $|\theta - \beta + k\Omega| < \alpha$ (d sections) and 0 for the rest of FS (nd-sections). Here, k is an integer number, and β is a mismatch angle between the nearest positive superconducting lobe and the reference CDW sector (in this work we restrict ourselves to the case $\beta = 0°$ corresponding to the $d_{x^2-y^2}$-wave order parameter symmetry inherent to cuprates). The parameter $\Omega = \pi/2$ and π for $N = 4$ and 2, respectively. The actual dielectric order parameter on the two-dimensional FS can be factorized as $\bar{\Sigma}(T,\theta) = \Sigma(T) f_\Sigma(\theta)$, where $\Sigma(T)$ is the T-dependent CDW order parameter, a solution of the self-consistent gap equation system [19,35,36,67,68].

The pseudogap experimental data [19,32–47] , seem to argue for the steep edges of CDW sector on the FS. Nevertheless, the d-wave behavior of the $\Sigma(k)$ dependence also remains on agenda [101]. If the latter scenario is true, the results obtained would not differ qualitatively. Therefore, to distinguish between those two possibilities, it is easier to directly lean upon precise experimental (e.g., ARPES) data.

Now, we can express the d-wave superconducting order parameter profile over the FS in the form similar to that

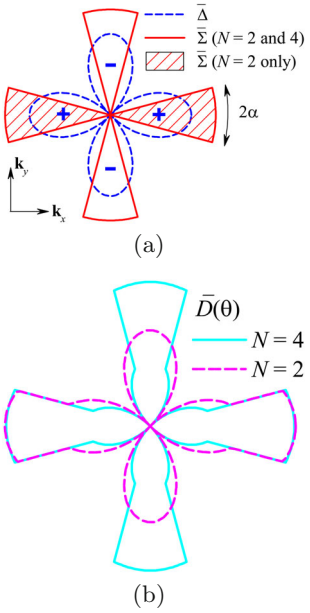

Fig. 1. (a) Profiles of the superconducting, $\bar{\Delta}(\theta)$, and dielectric, $\bar{\Sigma}(\theta)$, order parameters over the Fermi surface of the partially gapped d-wave charge-density-wave (CDW) superconductor. N is the number of CDW sectors with the width 2α each. (b) The corresponding energy-gap contours (gap roses).

for the CDW order parameter, i.e. $\bar{\Delta}(T,\theta) = \Delta(T) f_\Delta(\theta)$. The function $\Delta(T)$ is the T-dependent magnitude of the superconducting gap and the angular factor $f_\Delta(\theta)$ looks like $f^d_\Delta(\theta) = \cos 2(\theta - \beta)$ in the momentum space. In the related case of extended s-wave symmetry, the angular function has the form $f^{s^{\rm ext}}_\Delta(\theta) = |\cos 2(\theta - \beta)|$. The FS d-sections are characterized by the total gap

$$\bar{D}(T,\theta) = \sqrt{\bar{\Sigma}^2(T,\theta) + \bar{\Delta}^2(T,\theta)},$$

whereas $\bar{D}(T,\theta) = \bar{\Delta}(T,\theta)$ on the nd-sections. Quasiparticles demonstrate a Fermi-liquid behavior in the nodal region [103] in contrast to the anti-nodal one with the hot-spot deformation of the Fermi arc [60,104,105], which corresponds to $\beta = 0$. The profiles of the order parameters spanning the FS and the corresponding profiles of the energy gap (gap roses) are schematically illustrated in Figure 1.

It should be emphasized that our model is a generic one, whereas the observed CDWs are complex, sometimes develop differently on crystal surfaces and in the bulk [53], and, as is quite natural, are not identical for various high-T_c oxides. Nevertheless, the adopted model accounts for main features common to all materials concerned.

The dimensionless ratio $\sigma_0 = \Sigma_0/\Delta_0$, where Σ_0 and Δ_0 are the zero-T values of the corresponding order parameters in the absence of competing pairing, and the number of CDW sectors N, together with the temperature-independent angles α and β, compose a full set describing the CDW superconductor. In the further analysis, the parameter N and the superconducting pairing symmetry "sym" (sym = $d_{x^2-y^2}$, which will be hereafter denoted as d, and s) are assumed to be generic. Therefore, we

introduce the corresponding notation S^{sym}_{CDWN} for a partially gapped CDW superconductor. Pure s- and d-wave superconductors will be denoted as S^{s}_{BCS} and S^{d}_{BCS}, respectively. At the normalized temperature $t = T/\Delta_0$, the CDW superconductor is characterized by the order parameters $\sigma(t) = \Sigma(T)/\Delta_0$ and $\delta(t) = \Delta(T)/\Delta_0$.

Bearing this complexity in mind, it is no wonder that the stationary Josephson currents between CDW d-wave superconductors demonstrate peculiar angular dependences, which were studied earlier [41,66]. At the same time, the temperature and CDW-parameter dependences are no less interesting in view of detecting CDWs in cuprates and other related superconducting materials. To carry out corresponding calculations, we consider the same geometry as in our previous publications, specifically, restricting ourselves to the two-dimensional picture of tunneling, with the c-axes of electrodes being oriented in parallel to each other and to the junction plane.

The stationary Josephson critical current in the tunnel Hamiltonian approximation [4–6] is given by the formula [17,106,107]

$$I_c(T) = 4eT\sum_{\mathbf{pq}}\left|\widetilde{T}_{\mathbf{pq}}\right|^2\sum_{\omega_n}\mathsf{F}^{+}(\mathbf{p};\omega_n)\mathsf{F}'(\mathbf{q};-\omega_n). \qquad (1)$$

Here, $\widetilde{T}_{\mathbf{pq}}$ are the tunnel Hamiltonian matrix elements, $\mathbf{p}$ and $\mathbf{q}$ are the transferred momenta; $e > 0$ is the elementary electrical charge, and $\mathsf{F}(\mathbf{p};\omega_n)$ and $\mathsf{F}'(\mathbf{q};-\omega_n)$ are Gor'kov Green's functions for superconductors to the left and to the right, respectively, from the tunnel barrier (hereafter, all primed quantities are associated with the right hand side electrode). The internal summation is carried out over the discrete fermionic "frequencies" $\omega_n = (2n+1)\pi T$, $n = 0, \pm1, \pm2, \ldots$ The function $\mathsf{F}(\mathbf{p};\omega_n) \equiv \mathsf{F}_{CDWS}(\mathbf{p};\omega_n)$ corresponds to the CDW-gapped high-T_c oxide, whereas $\mathsf{F}'(\mathbf{q};\omega_n)$ describes either the identical high-T_c oxide ($\mathsf{F}'(\mathbf{q};\omega_n) \equiv \mathsf{F}'_{CDWS}(\mathbf{q};\omega_n)$) or an s-wave isotropic BCS superconductor ($\mathsf{F}'(\mathbf{q};\omega_n) \equiv \mathsf{F}'_{S^s_{BCS}}(\mathbf{q};\omega_n)$) with the order parameter $\bar{\Delta}_{sBCS}(T)$. Hence, we consider two representative cases: (i) the symmetric junction S^{sym}_{CDWN}-I-S^{sym}_{CDWN} involving identical high-T_c superconductors with an insulator interlayer I (sJ^{sym}_{CDWN}); and (ii) the non-symmetric S^{sym}_{CDWN}-I-S^{s}_{BCS} one (nJ^{sym}_{CDWN}, the S^{s}_{BCS} right hand side electrode is implied).

In the general case, the positive superconducting lobe of the CDWS to the left from the junction is oriented at the angle γ with respect to the normal $\mathbf{n}$ to the junction plane. In the symmetric junction, the same superconductor to the right from the junction can be oriented at a different angle, γ', with respect to the normal (see Fig. 2 for the sJ^{d}_{CDW4} junction). While tunneling, quasiparticles and Cooper pairs demonstrate directionality of two types. First, the multipliers $|\mathbf{v}_{g,nd}\cdot\mathbf{n}|$ and $|\mathbf{v}_{g,d}\cdot\mathbf{n}|$ appear [108–110], where $\mathbf{v}_{g,nd} = \nabla\xi_{nd}$ and $\mathbf{v}_{g,d} = \nabla\xi_{d}$ are the normal-state quasiparticle group velocities for proper FS sections. These multipliers can be factorized into $\cos\theta$, where θ is the angle at which the pair/quasiparticle transmits through the barrier, and a factor that can be incorporated into the

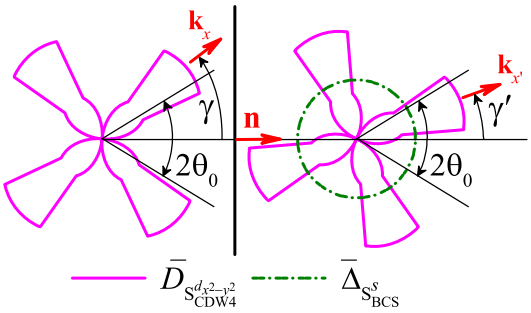

Fig. 2. Geometry of the Josephson junction. The left electrode is a CDW d-wave superconductor, whereas the right one can be either an identical CDW d-wave superconductor (the symmetric configuration) or a conventional s-wave superconductor (the non-symmetric configuration). See further explanations in the text.

junction normal-state resistance R_N [15,111–115]. Second, the tunnel matrix elements $\widetilde{T}_{\mathbf{pq}}$ in equation (1) become momentum-dependent [14,30,41,66,71,108–110,116–119], which differs from the assumption often used for isotropic superconductors [2,3].

Since the actual θ-dependences of $\widetilde{T}_{\mathbf{pq}}$ for realistic junctions are not known, we simulate the barrier-associated directionality by the phenomenological function

$$w(\theta) = \exp\left[-\left(\frac{\tan\theta}{\tan\theta_0}\right)^2\ln 2\right], \qquad (2)$$

so that the effective opening of relevant tunnel angles equals $2\theta_0$. The barrier transparency is normalized by the maximum value obtained for the normal tunneling with respect to the junction plane and included into the junction resistance R_N. Hence, $w(\theta = 0) = 1$. The multiplier $\ln 2$ in equation (2) was selected to provide $w(\theta = \theta_0) = \frac{1}{2}$.

As was already mentioned in Introduction, our approach is based on the assumption that the insulator layer I in the junction is so wide that the tunneling Hamiltonian approach is appropriate [89,90]. We also consider the original sinusoidal Josephson relationship between the actual stationary Josephson current I_J and the difference φ between the superconducting order parameter phases on both sides of the junction [2,3,107,120],

$$I_J(T) = I_c(T)\sin\varphi. \qquad (3)$$

Equation (3) holds true for isotropic s-wave superconductors. At the same time, the situation is much more involved for non-conventional ones, especially when the order parameter changes its sign while spanning over the FS [90,121]. This is believed to happen, e.g., in high-T_c oxides where the $d_{x^2-y^2}$-wave superconductivity manifests itself both in phase-insensitive [122] and phase-sensitive experiments [107,121,123].

It should be noted that the relation $I_J(\varphi)$ is no longer sinusoidal in various weak-link junctions such as constrictions or S-N-S structures (N is the normal metal) even in the s-wave case [89,90,124–126]. The influence

of Andreev-Saint-James reflection at the S-N boundary (boundaries) [90,107,115,121,127–132] constitutes a physical background of deviations from the Ambegaokar-Baratoff scenario [2,3], the latter leading to equation (3) and a monotonic convex curve $I_c(T)$. Those effects are totally neglected here because, from the very beginning, we assume the Blonder-Tinkham-Klapwijk parameter [129] $Z \gg 1$, so that Andreev-Saint-James levels inside the barrier are absent and the d-wave superconducting order parameter suppression [121] near the interlayer does not take place.

The explicit expressions for anomalous Gor'kov Green's functions for d- or extended s-wave superconductors, which enter (1), can be found elsewhere [41,66]. As a result, a standard – for the adopted case of coherent tunneling [14,30,64] – procedure [17,106] leads to the following formula for the dc Josephson current across the tunnel junction:

$$I_c(T,\gamma,\gamma') = \frac{1}{2eR_N} \times \frac{1}{\pi}\int_{-\pi/2}^{\pi/2} \cos\theta\; W(\theta)\; P(T,\theta,\gamma,\gamma')d\theta, \quad (4)$$

where [7,79]

$$P(T,\theta,\gamma,\gamma') = \bar{\Delta}\bar{\Delta}' \int\limits_{\min\{\bar{D},\bar{D}'\}}^{\max\{\bar{D},\bar{D}'\}} \frac{\tanh\frac{x}{2T}dx}{\sqrt{\left(x^2-\bar{D}^2\right)\left(\bar{D}'^2-x^2\right)}}. \quad (5)$$

Here, for brevity, we omitted the arguments in the dependences $\bar{\Delta}(T,\theta-\gamma)$, $\bar{\Delta}'(T,\theta-\gamma')$, $\bar{D}(T,\theta-\gamma)$, and $\bar{D}'(T,\theta-\gamma')$. Integration over θ is carried out within the interval $-\frac{\pi}{2} \le \theta \le \frac{\pi}{2}$, i.e. over the "FS hemicircle" turned towards the junction plane. If any directionality and CDW gapping are excluded, the integration over θ is absent and the angular factors f_Δ and f'_Δ remain preserved, we arrive at the Sigrist-Rice model [133].

3 Results of calculations and discussion

In the previous section, in order to reduce the number of energy-dependent problem parameters (Δ, Σ, and T), we carried out their *normalization* by the parameter Δ_0. With the same purpose in view while analyzing the Josephson current amplitude I_c, we introduce the dimensionless combination $i_c = I_c eR_N/\Delta_0$.

For further purposes, it is convenient to introduce other normalizations of the quantities concerned as well. For the temperature, it is the quantity $\tau = T/T_{c,\max}$, where $T_{c,\max}$ means the critical temperature for the whole junction; for $\mathrm{sJ}^{\mathrm{sym}}_{\mathrm{CDW}N}$ junctions, it is the critical temperature T_c of the CDW superconductor; but for $\mathrm{nJ}^{\mathrm{sym}}_{\mathrm{CDW}N}$ ones, it is the critical temperature of the $\mathrm{S}^s_{\mathrm{BCS}}$ electrode, because, in agreement with the observed ratios between the T_c's of cuprates and conventional metals, we select it to be lower than the critical temperature of CDW superconductor. We shall refer to the quantity τ as the "reduced temperature". When using this parameter, we should bear in mind that, in the case of CDW superconductors, the critical temperature T_c depends not only on the parameter Δ_0, but on the other parameters (Σ_0, α, β, and N) as well. Therefore, the relationship between the *reduced* temperature τ and the *normalized* temperature $t = T/\Delta_0$ introduced above is not a simple proportionality.

Besides, for the amplitude of the superconducting order parameter Δ and the magnitude of the stationary Josephson current I_c, we also introduce normalization by the corresponding value that this quantity has when one of the control parameters (these are t, σ_0, and α) is zero. (One should pay attention that, for CDW superconductors, the last two cases mean a comparison with the state of the corresponding (i.e. possessing the same Δ_0) pure s- or d-wave superconductor.). The relevant quantities will also be referred to as *reduced* ones and will be denoted by a small bold letter, with its argument being included into braces. For instance, the notation $\boldsymbol{i}_c\{\alpha\}$ stands for $i_c(\alpha)/i_c(\alpha=0)$.

We will also check the correlation between the *reduced* Josephson current $\boldsymbol{i}_c$ and, in the case of symmetric junction, the squared *reduced* superconducting gap $\boldsymbol{\delta}$ or, in the case of non-symmetric junction, the product of *reduced* superconducting gaps $\boldsymbol{\delta\delta}'$, with the driving force of correlation being one of the control parameters x. For such a correlation, we will use the notation $\boldsymbol{i}_c\{x\}\boldsymbol{\delta}^2$ or $\boldsymbol{i}_c\{x\}\boldsymbol{\delta\delta}'$.

3.1 The law of corresponding states. Effect of tunnel directionality

Temperature dependences

From the aforesaid (see introduction), it is clear that the combination of two "universal" theories (the BCS theory in the weak-coupling approximation for the superconducting electrodes and the Bardeen approach for the tunnel Hamiltonian [5] – constant tunnel matrix elements and the neglect of tunnel directionality) must result in a "universal" normalized curve, the Ambegaokar-Baratoff one [2,3], which describes the dependence of the reduced Josephson current $\boldsymbol{i}_c$ on the reduced temperature τ (in our notation, $\boldsymbol{i}_c\{\tau\}$) in the case of the symmetric junction $\mathrm{sJ}^s_{\mathrm{BCS}}$. If we compare (see Fig. 3, solid curves) two "universal" dependences, $\boldsymbol{\delta}^2\{\tau\}$ for an $\mathrm{S}^s_{\mathrm{BCS}}$ superconductor and $\boldsymbol{i}_c\{\tau\}$ for an $\mathrm{sJ}^s_{\mathrm{BCS}}$ junction, we see that they are very similar, so that the relation between $\boldsymbol{i}_c$ and $\boldsymbol{\delta}^2$ is almost linear. We should by no means expect that such a behavior remains valid if one takes into account the possibility of Andreev-Saint-James reflections [127,128,131] due to the transition of junction interlayer from the dielectric into the metallic state, so that the dimensionless barrier strength becomes finite [129]. In this very important case, zero-energy states are formed, and a transition from 0- to π-junction as the temperature falls down is predicted giving rise to substantial distortions of the reference Ambegaokar-Baratoff $I_c(T)$ curves [115,121,134,135].

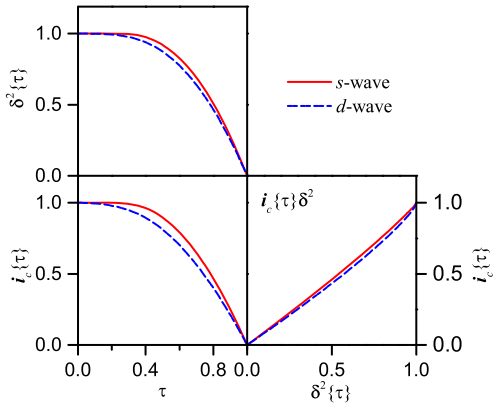

Fig. 3. Dependences of the reduced squared superconducting energy gap $\boldsymbol{\delta}^2$ and the reduced stationary Josephson current $\boldsymbol{i}_c$ on the reduced temperature τ (left panels), and the corresponding correlation $\boldsymbol{i}_c\{\tau\}\boldsymbol{\delta}^2$ (right panel) for symmetric tunnel junctions between pure s- and d-wave superconductors ($\mathrm{sJ}^{s,d}_{\mathrm{BCS}}$). The tunnel directionality is neglected ($\theta_0 = 90°$). See explanations in the text.

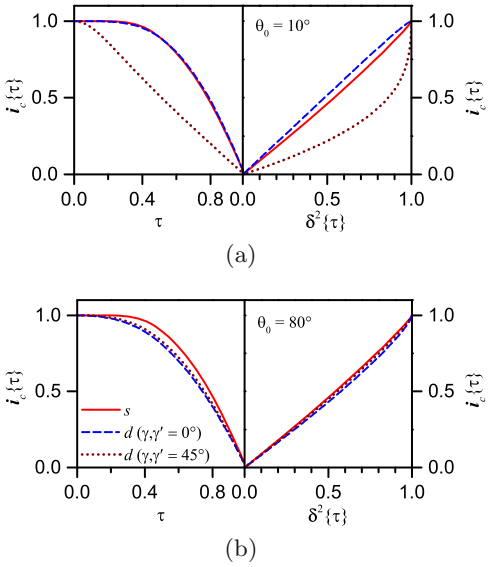

Fig. 4. Dependences of the reduced stationary Josephson current $\boldsymbol{i}_c$ on the reduced temperature τ (left panels) and the corresponding correlation $\boldsymbol{i}_c\{\tau\}\boldsymbol{\delta}^2$ (right panels) for $\mathrm{sJ}^{s,d}_{\mathrm{BCS}}$ with the electrode crystal lattices rotated by $\gamma = \gamma' = 0$ and 45° with respect to the normal $\mathbf{n}$ to the junction plane. The tunnel directionality parameter $\theta_0 = 10°$ (a) and 80° (b).

Although it is not known for sure whether the very Andreev-Saint-James reflection affects the Josephson current in cuprate-based structures, there is a certain evidence that the Ambegaokar-Baratoff behavior is violated for them. Significant deviations were reported, e.g., for underdoped intrinsic junctions made of (Hg,Re)$Ba_2Ca_2Cu_3O_{8+\delta}$ [136], $Bi_2Sr_2CaCu_2O_{8+\delta}$ [137], and $YBa_2Cu_3O_{7-\delta}$ [138], which are suspected to be of the S-N-S type, as well as for $YBa_2Cu_3O_{7-\delta}$ grain boundary [139,140], step-edge [141] and ramp-edge [142] junctions. The concave character of the $I_c(T)$ curve in certain T ranges instead of the convex Ambegaokar-Baratoff behavior was observed in the discussed experiments. The $0-\pi$-transition interpretation of the corresponding $I_c(T)$ data seems to be quite reasonable.

Returning to our model, which calls into play CDWs, the simplest scenario with no tunnel directionality cannot be applied for the calculation of I_c, e.g., through a symmetric or nonsymmetric junction, in which at least one electrode is the $\mathrm{S}^d_{\mathrm{BCS}}$ superconductor, because the sign-alternating character of the corresponding d-wave order parameter makes I_c equal to zero when integrating over the FS. Therefore, an introduction of additional factors like tunnel directionality and/or tunnel coherence, which include extra angular model parameters, becomes unavoidable. However, if we try to use the minimum number of extra assumptions – namely, coherent tunneling and zero misorientation between electrodes, i.e. $\gamma = \gamma'$ – the relationship between the current and the squared superconducting order parameter turns out almost the same (Fig. 3, right lower panel, dashed curve), i.e. close to the linear one. This fact gives us ground to suppose that, in the adopted simple model, the temperature affects the current magnitude mostly via changing the superconducting order parameter, irrespective of its pairing symmetry.

The proposed hypothesis can be verified by calculating the $\boldsymbol{i}_c$ dependences on $\boldsymbol{\delta}^2$ for junctions with varying model parameters of CDW superconductors. Below, we shall refer to them as the *corresponding-state dependences* (CSDs). The situation becomes even more interesting if we take into account that (i) the superconducting and dielectric order parameters have different pairing symmetries and (ii) the CDW superconductor gives a possibility to alter the magnitude of Δ by changing not only the temperature but also the parameters of FS dielectrization.

Hence, we may assert that the law of corresponding states holds true with rather a good accuracy if the tunnel directionality is not taken into account. However, making allowance for this factor changes the situation drastically. In Figure 4, the dependences $\boldsymbol{i}_c\{\tau\}$ are shown for $\mathrm{sJ}^s_{\mathrm{BCS}}$ and $\mathrm{sJ}^d_{\mathrm{BCS}}$ junctions, with the $\mathrm{S}^d_{\mathrm{BCS}}$ superconductors in the latter being oriented at the angles $\gamma = \gamma' = 0°$ or 45° with respect to the normal. In panel (a), the plots were calculated for $\theta_0 = 10°$, i.e. for a rather strong directionality. One sees that the orientation of the anisotropic $\mathrm{S}^d_{\mathrm{BCS}}$ superconductor substantially affects the results. The maximum effect is attained when the FS section that dominates in tunneling includes Δ-nodes ($\gamma = \gamma' = 45°$). At the same time, if the Δ-nodes are located beyond the effective tunneling cone (i.e. for $\gamma = \gamma' = 0°$), the $i_c(\tau)$ curves for the s- and d-wave cases are rather close. It is so because the spread of the d-wave gap lobe in the cone $2\theta_0$ is rather narrow at $\theta_0 = 10°$, and the "tunnel-active" FS section can be regarded as if Δ were isotropic. When the directionality decreases, i.e. the parameter θ_0 grows (see panel (b) for $\theta_0 = 80°$), the effect diminishes, and the d-wave curves tend to their common limit depicted in Figure 3 (dashed curves).

Although the actual magnitude of the parameter θ_0 is unknown, its smaller values are more probable than larger ones. Indeed, for the assumed coherent tunneling calculated, say, in the Wentzel-Kramers-Brillouin (WKB) approximation [143], which is valid at least for thick enough interlayers, the penetration coefficient is proportional to $\exp(-h_b d)$, where h_b is the effective barrier height for the particle (pair), $d = L/\cos\theta$ is the relevant tunnel path, and L is the junction thickness. Therefore, the plots in Figure 4a, which correspond to thicker junctions, seem to be more realistic than those shown in Figure 4b. It means that for cuprates, whatever the symmetry of their superconducting order parameter(s), the Ambegaokar-Baratoff-like dependence $I_c(T)$ and the proportionality between $\boldsymbol{i}_c\{t\}$ and $\boldsymbol{\delta}^2\{t\}$ should be observed in symmetric junctions. Should this simple relation appropriate to the basic model be spoiled, there must be sound physical factors responsible for that. On the basis of our previous studies [19,32–34,41,66,68–71,81,82,144,145], we propose CDWs as a candidate.

3.2 Symmetric junctions

3.2.1 Checkerboard CDW configuration

To detect CSD violations and bearing in mind the results obtained in Section 3.1, various dependences for the Josephson current in the symmetric junction will be calculated for the tunnel directionality parameter $\theta_0 = 10°$. We shall start from the simplest case for electrode orientations, $\gamma = \gamma' = 0$.

Figure 5 illustrates that the law of corresponding states is satisfied with a rather good accuracy in all practically important considered cases of $\mathrm{sJ}^d_{\mathrm{CDW4}}$ junctions. This is the more so interesting because every of those panels demonstrates a specific feature associated with the availability of CDWs. In particular, the change of the parameter σ_0 in panel (a) substantially deforms the $\boldsymbol{i}_c\{\alpha\}$ profiles, but the relevant CSDs $\boldsymbol{i}_c\{\alpha\}\boldsymbol{\delta}^2$ remain close to one another. To a great extent, this situation takes place owing to the fact that all junction states, in which CDWs are completely suppressed by superconductivity, are mapped onto a single point (1,1) in the reduced coordinates. Panels (b) and (c) illustrate that the law of corresponding states is also obeyed rather well if either the degree of FS dielectrization or the temperature, respectively, affects the superconducting order parameter.

At the same time, some $\boldsymbol{i}_c\{x\}\boldsymbol{\delta}^2$ dependences with $x = \sigma_0$ or α in panels (a) and (b) reveal a singular-like behavior in the range of small δ's. This is especially noticeable for the $\alpha = 5°$-curve in the right panel (b). Such behavior can also be observed in other CSDs considered below and requires a special analysis (see Appendix). Figure A.1a in Appendix also enables one to get convinced that the $i_c(\alpha, \sigma_0 = \text{const})$ dependences on panel (a) and the $i_c(\sigma_0, \alpha = \text{const})$ in panel (b) strongly resemble the corresponding dependences of the parameter $\delta(0)$, which are the cross-sections of the surface $\delta(0)$ versus (σ_0, α) depicted in this figure.

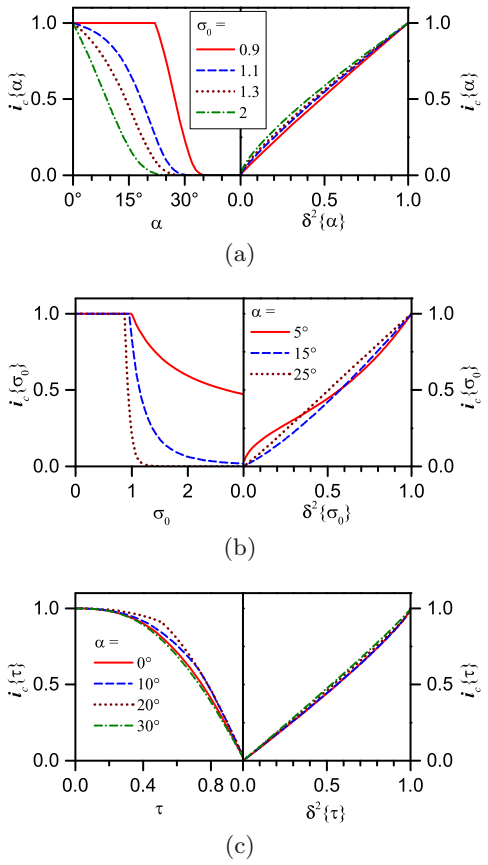

Fig. 5. (Left panels) Dependences of the reduced stationary Josephson current $\boldsymbol{i}_c$ on (a) the degree of the Fermi surface (FS) dielectric gapping α for various ratios σ_0's between the strengths of Cooper and electron-hole pairings at the temperature $T = 0$, (b) σ_0 for various α's at $T = 0$, and (c) τ for various α's at $\sigma_0 = 1.3$, and the corresponding correlations $\boldsymbol{i}_c\{x = \alpha \text{ or } \sigma_0\}\boldsymbol{\delta}^2$ (right panels) for symmetric tunnel junctions between d-wave superconductors with checkerboard charge-density waves ($\mathrm{sJ}^d_{\mathrm{CDW4}}$). The tunnel directionality parameter $\theta_0 = 10°$; $\gamma = \gamma' = 0$. See explanations in the text.

In their turn, the dependences $\boldsymbol{i}_c\{\tau\}$ reveal peculiarities associated with the CDW reentrance in a certain temperature interval [36]. In panel (c), they are the most noticeable in the $\alpha = 10°$- and $\alpha = 20°$-curves, being effectively smoothed out in the CSDs (see below).

A simple examination of Figures A.1 and A.2 makes it evident that even the zero-temperature values of the order parameters, $\Delta(T = 0)$ and $\Sigma(T = 0)$, may drastically differ from their parent values Δ_0 and Σ_0. The situation becomes even more involved at finite T's and, at first glance, paradoxical, if we try to carry out the CSD verification. In the framework of ideology of corresponding states, we should calculate the required I_c and Δ values, including the normalizing ones (taken at $T = 0$), at a certain reduced temperature τ. In Figures 6a and 6b, we demonstrate the $\boldsymbol{i}_c\{\sigma_0\}$ and $\boldsymbol{i}_c\{\alpha\}$ dependences, respectively, and the corresponding CSDs calculated for $\tau = 0.7$. The revealed nonmonotonic behavior is a direct consequence of

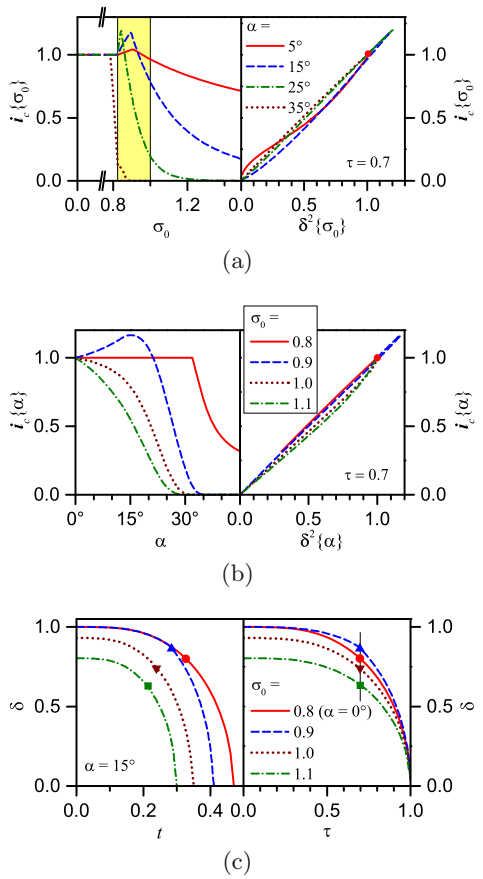

Fig. 6. (a) and (b) The same as in Figures 5b and 5a, but at the finite reduced temperature $\tau = 0.7$. (c) Explanation of the non-monotonic behavior of the $\boldsymbol{i}_c\{\alpha\}$ dependence in the reentrance region (the curve $\sigma_0 = 0.9$ in panel (b)). See further explanations in the text.

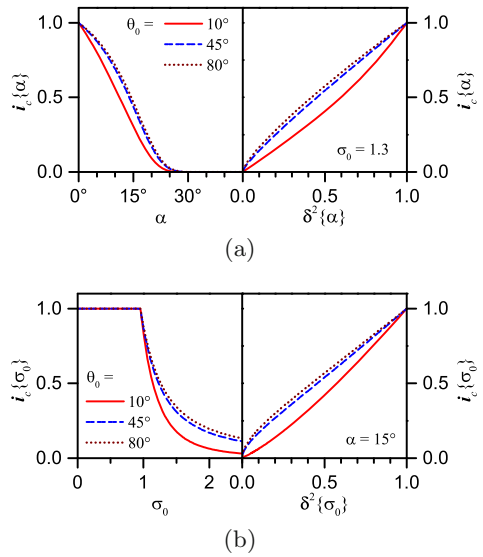

Fig. 7. (Left panels) Dependences (a) $\boldsymbol{i}_c\{\alpha\}$ at $\sigma_0 = 1.3$ and (b) $\boldsymbol{i}_c\{\sigma_0\}$ at $\alpha = 15°$ for various θ_0's for $\mathrm{sJ}^d_{\mathrm{CDW4}}$ junctions. $T = 0$, $\gamma = \gamma' = 0$. (Right panels) The corresponding correlations $\boldsymbol{i}_c\{x = \alpha \text{ or } \sigma_0\}\boldsymbol{\delta}^2$.

CDWs or, to be more precise, the Σ reentrance effect. In panel (c), a relevant explanation for the curves in panel (b) is given.

Indeed, at $\alpha = 15°$ and $\sigma_0 = 0.9$, CDWs are suppressed below a certain temperature T_1 [35,36,41,67–69]. Up to this temperature, the dependence $\Delta(T < T_1)$ coincides with that for a pure $\mathrm{S}^d_{\mathrm{BCS}}$ superconductor (this is the interval in the left panel (c), where the $\alpha = 15°$ curve and its reference one ($\alpha = 0°$) overlap. At $T > T_1$, the emerging CDW effectively suppress superconductivity. In particular, it considerably reduces T_c and makes the $\Delta(T)$-slope steeper (see illustrative plots in works [68,69]). As a result, the reduced $\boldsymbol{i}_c\{\tau\}$ dependence for the $\mathrm{sJ}^d_{\mathrm{CDW4}}$ junction passes above the corresponding dependence for the $\mathrm{sJ}^d_{\mathrm{BCS}}$ one, with a cusp at the point of CDW emergence. (Such cusps could already be noticed in Fig. 5c.). The $\boldsymbol{i}_c$-ordinate of the point with the abscissa $\tau = 0.7$ in the $\alpha = 0°$ curve (marked by a circle) serves as a normalizing value for the $\boldsymbol{i}_c$-ordinate of the point with the same abscissa in the $\alpha = 15°$ curve (marked by a triangle), which makes their ratio larger than unity. The left panel (c) illustrates how all that looks like in the "normalized" (not "reduced"!) coordinates. The parameter sets ($\alpha = 15°, \sigma_0 = 1$) and ($\alpha = 15°, \sigma_0 = 1.1$) are located beyond the reentrance region in the phase plane [35,36,41]. The temperature intervals of CDW existence for them extend down to $T = 0$, so that the CDW begins to suppress Δ starting from the zero temperature. As a result, the corresponding $\Delta(T)$-profiles become squeezed more uniformly in comparison with the reentrance case and the reduced $\boldsymbol{\delta}\{\tau\}$ and $\boldsymbol{i}_c\{\tau\}$ dependences lie below the reference ones, and the discussed non-monotonic behavior disappears.

An analogous explanation can also be given to the non-monotonic behavior observed in the $\boldsymbol{i}_c(\sigma_0)$ curves for a "reentrance" set of parameters. In the left panel (a), the "reentrance" interval of parameter σ_0 is painted. The figure makes it evident that all non-monotonic scenarios are inherent to the reentrance region only. It should be noted that the reentrance region is marked in the panel very schematically. In reality [35,36,41], its maximum width is attained at $\alpha = 0°$, and the reentrance takes place (not exactly because $\alpha = 0°$ means a pure $\mathrm{S}^d_{\mathrm{BCS}}$ superconductor, irrespective of σ_0-value) within the interval $\frac{\sqrt{e}}{2} < \sigma_0 < 1$ (it is this interval that is shown in the panel). As the angle α grows, this interval first gets narrower (mainly from the right side) and, starting from about $\alpha = 27°$, also slowly shifts to the left; at $\alpha = 45°$, the interval collapses into the point $\sigma_0 = \frac{1}{2}$. In Appendix (see Fig. A.1b), we marked the boundaries of the reentrance region by bright lines.

As was noticed above and shown in Figure 4, the weakening of directionality favors the investigated law of corresponding states. It can be directly illustrated by plotting the correlation $i_c\{\alpha\}\delta^2$ for various θ_0's (see Fig. 7a). One can see that the Ambegaokar-Baratoff-like behavior is restored at $\theta_0 \to 90°$. The same is true for the $i_c\{\sigma_0\}\delta^2$ dependence as is shown in Figure 7b.

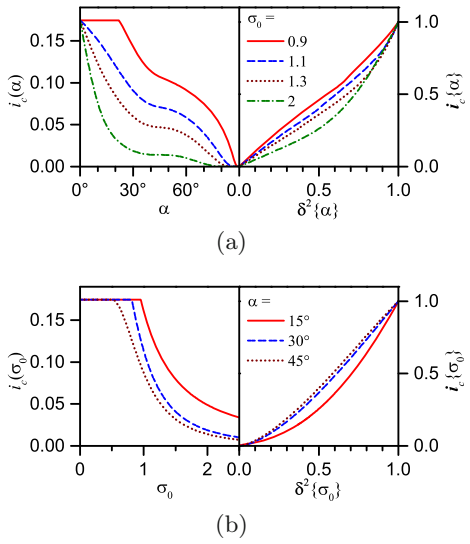

Fig. 8. (Left panels) The dependences of the normalized current (a) $i_c(\alpha)$ for various σ_0's and (b) $i_c(\sigma_0)$ for various α's for $\mathrm{sJ}^d_{\mathrm{CDW2}}$ junctions. $T = 0$, $\gamma = \gamma' = 0$, $\theta_0 = 10°$. (Right panels) The corresponding correlations $\boldsymbol{i}_c\{x = \alpha \text{ or } \sigma_0\}\boldsymbol{\delta}^2$.

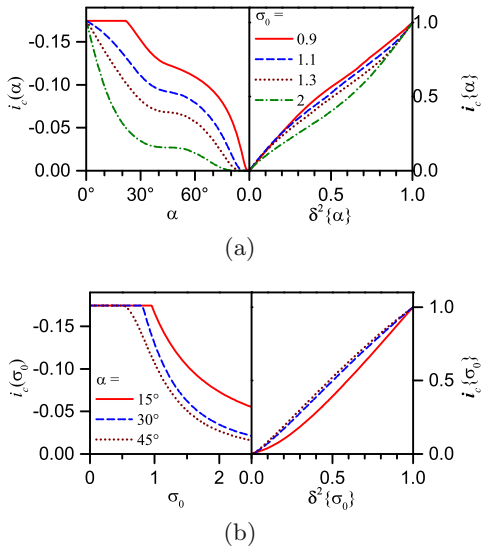

Fig. 9. The same as in Figure 8, but for $\gamma = 90°$ and $\gamma' = 0$. The ordinate axis is directed downwards.

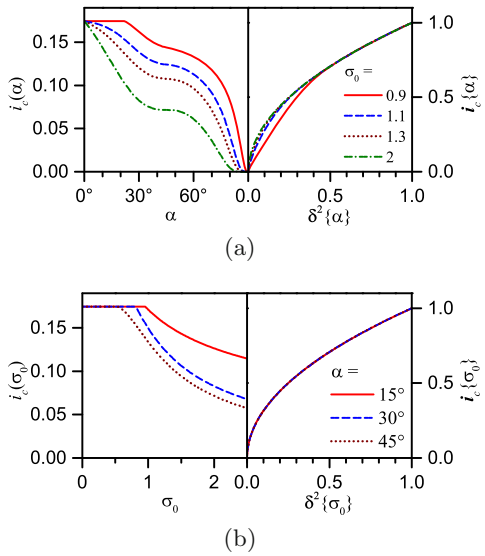

Fig. 10. The same as in Figure 8, but for $\gamma = \gamma' = 90°$.

3.2.2 Unidirectional CDW configuration

The CDW-driven deviations from the law of corresponding states become more conspicuous if one considers the case of $\mathrm{sJ}^d_{\mathrm{CDW2}}$ junction between $\mathrm{S}^d_{\mathrm{CDW2}}$ superconductors with unidirectional CDWs. The dependences $\Delta(\alpha)$ at fixed σ_0's demonstrate a specific "wavy" behavior differing from that in the checkerboard case (see Fig. A.2a in Appendix) [19,35,36,41]. From Figure 8a (here, the orientations of CDW-sector pairs in both electrodes are selected to be normal to the junction plane), we see that the waviness is reproduced in the $i_c(\alpha)$ dependences, although the CSDs $\boldsymbol{i}_c\{\alpha\}\boldsymbol{\delta}^2$ are deformed comparatively weakly. The case, when CDWs in the left $\mathrm{S}^d_{\mathrm{CDW2}}$ electrode are oriented in parallel to the junction plane, whereas the orientation of CDWs in the right $\mathrm{S}^d_{\mathrm{CDW2}}$ electrode remains the same, demonstrates a similar behavior as is seen from Figure 9a. Note, that i_c changes its sign in comparison to the previous electrode configuration, i.e. we arrive at a π-junction due to the alternating signs of the dominant superconducting lobes in both electrodes [41,66]. At the same time, when both CDW sectors are oriented along the junction plane, the CSD is violated, the deviations from linearity being quite different from those appropriate to other configurations (see Fig. 10a). The differences between $i_c(\sigma_0)$ dependences for the analyzed configurations in $\mathrm{sJ}^d_{\mathrm{CDW2}}$ junctions are analogous to those for $i_c(\alpha)$, as can be seen from Figures 8b, 9b, and 10b.

Hence, it comes about that the case of unidirectional CDWs is more favorable for observing deviations from the law of corresponding states.

Similarly to what was found above for the checkerboard CDW pattern, the strengthening of the directionality for $N = 2$ leads to more spectacular CSD violations. It is demonstrated in Figures 11a and 11b displayed for α and σ_0 dependences, respectively.

3.2.3 Rotated junction configurations

So far, we studied examined the CSDs for the reference Josephson junction configuration (with the electrodes oriented at $\gamma = \gamma' = 0$). On the other hand, other experimental configurations can be fabricated easily [146,147], giving more opportunities to study the phenomenon concerned. Therefore, it is worthwhile to analyse CSDs for different cases of rotated electrodes.

As an example, we chose the second electrode to be rotated by the angle $\gamma' = 45°$. In this case, the positive and negative contributions to the overall current i_c from the fragments of adjacent superconducting lobes that fall within the cone of effective tunneling mutually compensate each other provided that the left hand side electrode is oriented at $\gamma = 0°$. The other γ-values will result in

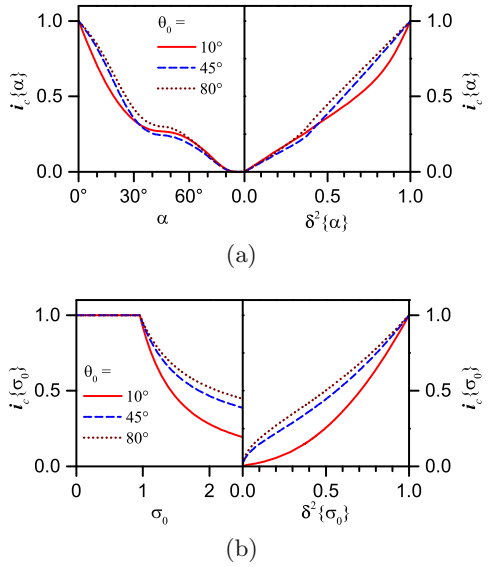

Fig. 11. The same as in Figure 7, but for sJ^d_{CDW2} junctions.

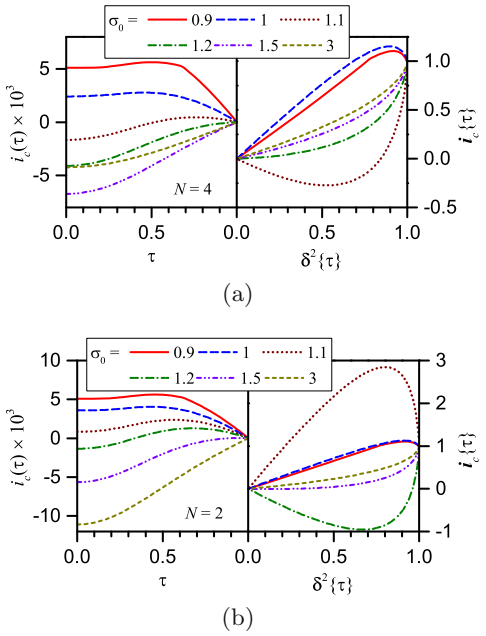

Fig. 12. (Left panels) The normalized $i_c(\tau)$ dependences for sJ^d_{CDW2} junctions at $\alpha = 15°$ and various σ_0's for $N = 4$ (a) and 2 (b). $\gamma = 15°$, $\gamma' = 45°$, $\theta_0 = 10°$. (Right panels) The corresponding correlations $\boldsymbol{i}_c\{\tau\}\boldsymbol{\delta}^2$.

non-zero currents. Hence, such a configuration can play the role of differential detector of various gap features on the FS of the left hand side electrode. Bearing in mind the distributions of both order parameters and the combined gap (the gap rose [36]) over the FS, it is reasonable to expect that the most noticeable effect will take place if the left hand side electrode is rotated by the angles $\gamma = \alpha$ or $\gamma = \theta_0$.

Now, by varying the angle γ, we can change the weights and even the signs of contributions to the total current from dielectrized and non-dielectrized FS sections. This makes it possible – although this is a very complicated task! – to trace minor variations in the temperature-dependent contributions from both order parameters having different symmetries. The results given below demonstrate that the obtained dependences are very sensitive to the problem parameters. We must also take into account the model approximations. Therefore, these results have only an illustrative meaning, but may be useful for experimenters when designing the experimental setup.

The calculated $i_c(\tau)$ plots and the corresponding $\boldsymbol{i}_c\{\tau\}\boldsymbol{\delta}^2$ dependences for the checkerboard CDW pattern ($N = 4$) are shown in Figure 12a for $\alpha = 15°$ and various σ_0. One sees that the temperature CSDs are severely violated for rotated crystals. Such an experimental setup is very easy to perform: to find the effect it is enough to change the temperature T and the rotation angle for the *same crystal* during the process of measurements. Note that the magnitudes of the currents becomes small as compared to the case $\gamma = \gamma' = 0$, when the lobes in both electrodes are oriented along the normal to the junction, $\mathbf{n}$. "Switching on" the CDWs leads to a considerable distortion of the CSD, thus confirming the high sensitivity of this "differential" scheme to the system parameters.

The effect is even stronger for unidirectional CDWs ($N = 2$) as can be inferred from Figure 12b displaying the results of calculations for the same set of parameters. Huge CSD violations should be detected when σ_0 is close to unity, i.e. when the Cooper and electron-hole pairing strengths are comparable. This situation is expected for the doping values y's not far away from the optimum one, when the pseudogap-temperature curve on the cuprate T-y phase diagram crosses the superconducting dome [38,148,149].

The same dependences but for the fixed $\sigma_0 = 1.3$ and various α's are depicted in Figure 13a. One can see that, in the absence of CDWs ($\alpha = 0$), the CSDs are slightly violated. The growth of α makes violations stronger, especially when α becomes equal to $\theta_0 = 10°$. The subsequent increase of α leads to the decrease of violations, so that finally the CSDs become obeyed even much better than in the absence of CDWs. This results means that, in order to check the presented theory, it would be desirable to measure the Josephson current for a number of high-T_c samples with different oxygen content.

Again, the deviations from the CSDs with the increasing α are more pronounced in the case $N = 2$, which is demonstrated in Figure 13b. The appearance of the pseudogap (CDWs) on the antinodal FS sections results in strong deviations from the corresponding state law, with respect to not only the magnitude but also the sign. In particular, for $\alpha \approx \theta_0$, the plot $\boldsymbol{i}_c\{\tau\}\boldsymbol{\delta}^2$ has nothing to do with the CSD.

Hence, irrespective of whether the CSDs hold true, the $i_c(\tau)$ dependences are interesting by themselves, because CDWs – in addition to the Andreev-Saint-James-reflection effect [115,121,134,135] – can also induce violations of Ambegaokar-Baratoff relations for cuprate-based

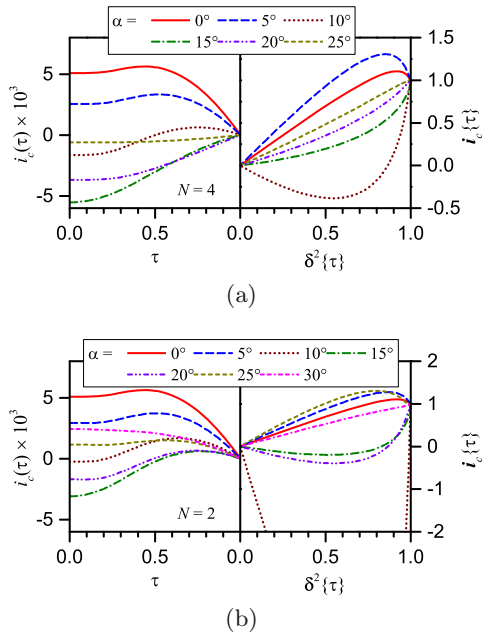

Fig. 13. The same as in Figure 12, but for various α's at $\sigma_0 = 1.3$.

junctions. Therefore, measurements of $i_c(\tau)$ at varying γ and γ' may reveal the CDW existence in cuprate samples.

One can imagine another reason that may influence the angular dependences of i_c, namely, it is a possible oxygen depletion at high-angle grain boundaries found in $YBa_2Cu_3O_{7-\delta}$ bicrystal junctions [150]. This circumstance might impede the experimental identification of the rotation effects resulting from coherent and direction-dependent tunneling.

3.3 Non-symmetric junctions

Calculations for non-symmetric junctions nJ^{sym}_{CDWN} were carried out assuming the right hand side electrode to be an S^s_{BCS} superconductor with the isotropic superconducting gap. Concerning the specific value of the parameter Δ'_{BCS}, if the CDW superconductor is, say, $Bi_2Sr_2CaCu_2O_{8+\delta}$, and niobium is chosen as a counter-electrode, then $\Delta'_{BCS}(T=0) \approx 0.1\Delta_0$ (the gap is compared with the parameter Δ_0 of the counterpart S_{CDWN} electrode!), and we select the dimensionless parameter $\delta'_{BCS} = 0.1$. Owing to such a large difference between the order parameter magnitudes in both electrodes, the parameter Δ, as well as Σ, remains almost constant within the temperature interval where the parameter Δ' and, accordingly, the current i_c are non-zero. Therefore, the temperature dependence of the Josephson current is mainly determined by the gap function $\Delta'_{BCS}(T)$ inherent to the conventional S^s_{BCS} superconductor with much smaller T_c than that of the high-T_c oxide. Any investigation of the CDW influence on the correlations $\boldsymbol{i}_c\{\tau\}\boldsymbol{\delta\delta'}$ would give rise to the results similar to those depicted in Figure 3 for junctions with pure S^s_{BCS} electrodes.

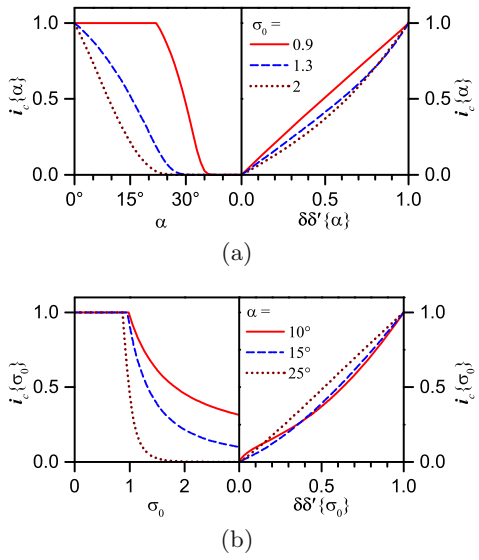

Fig. 14. (Left panels) The same as the left panels in Figures 5a and 5b, but for non-symmetric nJ^d_{CDW4} junctions. (Right panels) The corresponding correlations $\boldsymbol{i}_c\{x = \alpha \text{ or } \sigma_0\}\boldsymbol{\delta\delta'}$.

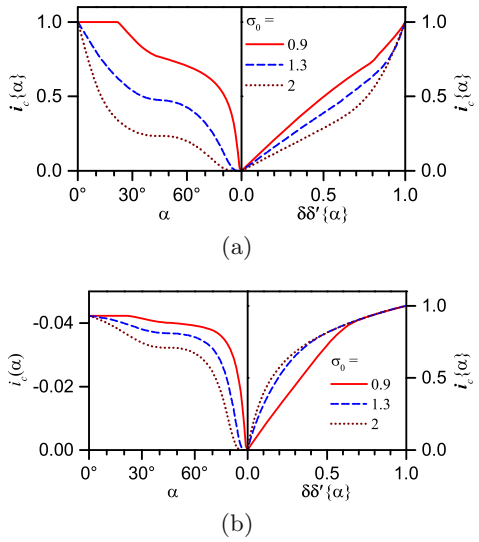

Fig. 15. (Left panels) The dependences (a) $\boldsymbol{i}_c\{\alpha\}$ at $\gamma = 0$ and (b) $i_c(a)$ at $\gamma = 90°$ for various σ_0's for nJ^d_{CDW2} junctions. $T = 0$, $\theta_0 = 10°$. (Right panels) The corresponding correlations $\boldsymbol{i}_c\{\alpha\}\boldsymbol{\delta\delta'}$.

In Figure 14, the correlations $\boldsymbol{i}_c\{x\}\boldsymbol{\delta\delta'}$ are shown for $x = \alpha$ (panel (a)) and σ_0 (panel (b)). Here, CDWs in the $d_{x^2-y^2}$-wave superconductor were assumed to possess the checkerboard configuration ($N = 4$), and the other parameters are $\theta_0 = 10°$ and $\gamma = 0°$. Conspicuous deviations from the law of corresponding states are readily seen.

The dependences analogous to those depicted in Figure 14b are shown in Figure 15a for unidirectional CDWs ($N = 2$). The violations of the proportionality in the dependence $\boldsymbol{i}_c\{x\}\boldsymbol{\delta\delta'}$ become substantially stronger than for $N = 4$. In Figure 15b, the results of the same calculations as in panel (a), but for the rotated cuprate crystal,

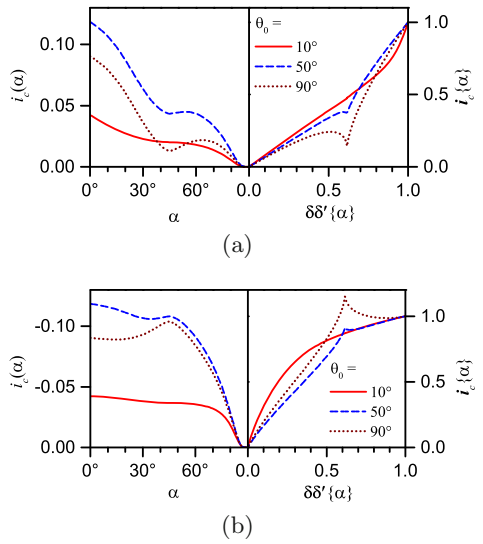

Fig. 16. (Left panels) The dependences $i_c(\alpha)$ for $\sigma_0 = 1.3$ and various θ_0's for $\mathrm{nJ}^d_{\mathrm{CDW2}}$ junctions with the orientations $\gamma = 0$ (a) and 90° (b). $T = 0$. (Right panels) The corresponding correlations $\boldsymbol{i}_c\{\alpha\}\boldsymbol{\delta\delta'}$.

$\gamma = 90°$, are demonstrated. The left hand side of panel (b) exhibits the dependence $i_c(\alpha)$ rather than $\boldsymbol{i}_c\{\alpha\}$ to illustrate that the current changed its sign, because in this case the superconducting lobes with opposite signs overlap (nevertheless, for the sake of convenience, we inverted the ordinate axis). It is obvious that the law of corresponding states is no longer valid for this π-junction.

Thus, the proportionality observed in the CDW-free case may be violated by CDWs even in the case of thick interlayers (strong directionality) where the compensation between current components of opposite signs is minimal. This is much more true for thinner inter-electrode distances, when θ_0 is larger. Figure 16a illustrates the results of calculated correlations $\boldsymbol{i}_c\{\alpha\}\boldsymbol{\delta\delta'}$ for $N = 2$, $\gamma = 0°$, and $\sigma_0 = 1.3$. The curves become severely distorted with growing θ_0, which is a direct result of the CDW influence. For $\gamma = 90°$, the violations of the law of corresponding states are also strong, as is shown in Figure 16b (the left ordinate axis is inverted).

Hence, one can see that the $\boldsymbol{i}_c\{x\}\boldsymbol{\delta\delta'}$ dependences in the non-symmetric case become more sensitive to the existence of CDWs at larger θ_0's, i.e. for more isotropic tunneling, in contrast to the symmetric junction. This behavior can be explained by the fact that at large θ_0's both positive and negative superconducting lobes make contributions to the total current. But in the case of symmetric junction, the overlap of the lobes with the same or the opposite signs give the contributions of the same sign to the total current. This current "rectification" does not take place in the non-symmetric configuration. In other words, we obtain a configuration that operates similarly to the "differential" setup described in Section 3.2.3, and therefore has a higher sensitivity to parameter changes.

It is worth noting that the non-symmetric configuration with the controllable spacing between electrodes is the same as that in scanning tunnel microscopy, but designed to measure the Josephson rather than the quasiparticle component of the tunnel current. Changing the distance between the electrodes corresponds to the variation of the angle θ_0.

4 Conclusions

It was shown that the stationary Josephson temperature-dependent current, $I_c(T)$, is almost proportional to the product of superconducting gap amplitudes $\Delta(T)\Delta'(T)$ for both electrodes in the cases of symmetric junction with s-wave and d-wave BCS superconductors as electrodes. The existence of such a proportionality, which can be considered as the law of corresponding states, was also studied for symmetric and non-symmetric junctions involving d-wave superconductors with CDWs, when the superconducting gap magnitude can be controlled not only by varying the temperature, but also the half-width α of the CDW sectors and the ratio σ_0 between the strengths of parent electron-hole and Cooper pairings. It turned out that this correlation may be strongly violated by checkerboard and, especially, unidirectional CDWs. Conditions were found, when the violations become more conspicuous to be observed experimentally. The temperature-driven (T is the parameter that can be varied the most easily) CSD violations caused by CDWs turned out to be reliably detected in properly designed symmetric junctions enhancing the sensitivity of the system to small variations of problem parameters. Also, the dependences on the angle α, which describes the extension of FS dielectric gapping and can be governed by doping, provides a test ground for detecting CDWs as a driving force violating the law of corresponding states. The non-symmetric configuration of the tunnel junction, when a counter electrode is an isotropic BCS superconductor, turned out to be sensitive to the CDW manifestations as well.

The reduced $I_c(T/T_c)$ dependences themselves were also shown to be substantially distorted by CDWs in comparison with Ambegaokar-Baratoff reference curves. The results strongly depend on the rotation angles γ and γ' of both crystal electrodes with respect to the junction plane. In certain T ranges $I_c(T/T_c)$ even becomes non-monotonic.

The results obtained have a general character and can be applicable not only to cuprates but also to other d-wave superconducting compounds with CDWs.

The study of the dc Josephson current and certain emerging correlations between measured quantities can help to detect CDWs in various superconductors. A variety of indirect methods intended to find CDWs in cuprates is necessary, because direct X-ray scattering may fail due to small amplitudes of CDW-induced distortions in CuO_2 planes [57]. At the same time, the temperature dependences of I_c, as well as the I_c-dependences on the CDW superconductor parameters α and σ_0, cannot unambiguously discriminate between the superconducting order parameters of different symmetry. To do this, one should measure, e.g., the angular dependences of the stationary

Josephson current measured in devices with different configurations [41,63,64,70,71,90,107,115,146,147,151,152].

The work was partially supported by the Project N 8 of the 2012–2014 Scientific Cooperation Agreement between Poland and Ukraine. MSL was also supported by the Narodowe Centrum Nauki in Poland (Grant No. 2011/01/B/NZ1/01622). The authors are grateful to Alexander Kasatkin and Alexander Kordyuk (Institute of Metal Physics, Kyiv) for useful remarks.

Appendix

In this Appendix, we restrict ourselves to estimations, so that the directionality factors $W(\theta)$ and $\cos\theta$ in formula (4) are omitted. Moreover, we will make estimations only for the "main" configuration of this work, the symmetric sJ^d_{CDW4} junction, in which the CDW sectors and the superconducting lobes of both electrodes are oriented in parallel to the junction normal ($\gamma = \gamma' = 0$). Then, the upper and lower limits of integral (5) converge, and we can easily obtain

$$P(T,\theta) = \frac{\pi}{2}\cos^2 2\theta \frac{\Delta^2(T)\tanh\dfrac{\bar{D}(T,\theta)}{2T}}{\bar{D}(T,\theta)}, \tag{A.1}$$

where $\bar{D}(T,\theta) = \sqrt{\Sigma^2(T)+\Delta^2(T,\theta)}$ on the dielectrized FS sections and $\bar{\Delta}(T,\theta)$ on the non-dielectrized ones. Hence, formula (4) reads

$$I_c(T) = \frac{\Delta(T)}{2eR_N}\left[\Delta(T)\int_0^\alpha \frac{\tanh\dfrac{\sqrt{\Sigma^2(T)+\Delta^2(T)\cos^2 2\theta}}{2T}}{\sqrt{\Sigma^2(T)+\Delta^2(T)\cos^2 2\theta}} \times \cos^2 2\theta\, d\theta + \int_\alpha^{\pi/4} \tanh\frac{\Delta(T)\cos 2\theta}{2T}\cos 2\theta\, d\theta\right]. \tag{A.2}$$

We see that one of the difficulties in calculating the Josephson current analytically even in our very simplified model consists in the hyperbolic tangent in the integrands of formula (A.2).

In the vicinity of T_c, $\Delta \to 0$, but in most cases $\Sigma(T_c) > 0$. Then,

$$I_c(T\to T_c) = \frac{\Delta^2(T)}{2eR_N} \times \left[\frac{\tanh\dfrac{\Sigma(T_c)}{2T_c}}{\Sigma(T_c)}\int_0^\alpha \cos^2 2\theta d\theta + \frac{1}{2T_c}\int_\alpha^{\pi/4}\cos^2 2\theta d\theta\right]. \tag{A.3}$$

On the other hand, at $T \to 0$, the function $\tanh\dfrac{x}{2T} \to 1$, and we obtain

$$I_c(T\to 0) = \frac{\Delta(0)}{2eR_N} \times \left[\Delta(0)\int_0^\alpha \frac{\cos^2 2\theta d\theta}{\sqrt{\Sigma^2(0)+\Delta^2(0)\cos^2 2\theta}} + \int_\alpha^{\pi/4}\cos 2\theta d\theta\right]. \tag{A.4}$$

The influence of $\Delta(0)$ in the denominator of the first intergrand is much weaker than that of the pre-integral $\Delta(0)$-factor, so that $I_c(T\to 0)$ can be regarded, with an accuracy sufficient for estimations, as a sum of a linear and a quadratic in $\Delta(0)$ term.

The zero-parameter value of I_c, which is used in this work for normalization, is obtained by putting one of the control parameters (T, Σ, α) equal to zero provided the others remaining fixed. In the case of parameters Σ and α, this means a comparison with a pure sJ^d_{BCS} case for which formula (A.4) gives ($\alpha \to 0$ and $\Delta(0) \to \Delta_0$).

$$I_c^0(0) = \frac{\Delta_0}{4eR_N}. \tag{A.5}$$

(We obtained a formula that differs from the case of sJ^s_{BCS} junction [3] by a factor of $\frac{1}{2}$. This is of no surprise because there is a cosine factor in the sJ^d_{BCS}-case.).

If the temperature T is selected as a control parameter, the situation is more involved. It is so because the value of $I_c(T=0)$ is governed by $\Sigma(0)$ and $\Delta(0)$ (see formula (A.4)). The latter are interdependent functions of model parameters and demonstrate a rather complicated behavior (see Fig. A.1, the profiles are observed from different directions). Attention should be paid to a close similarity between the $i_c(\alpha, \sigma_0 = \text{const})$ and $i_c(\sigma_0, \alpha = \text{const})$ dependences calculated at $t = 0$ and plotted in a number of figures in Section 3, on the one hand, and, on the other hand, the corresponding cross-sections of the $\delta(0)$-surface depicted in panel (a).

With the same illustrative purpose in view, in Figure A.2, we exhibit the (α, σ_0)-dependences of the normalized zero-temperature order parameters $\delta(0)$ and $\sigma(0)$ obtained in the case of S^d_{CDW2} superconductor. One can easily see (e.g., in Fig. 8) that the corresponding $i_c(\alpha, \sigma_0 = \text{const})$ dependences reproduce this "wavy" profile, but the CSDs $\boldsymbol{i}_c\{\alpha\}\boldsymbol{\delta}^2$ remain more or less close to the law of corresponding states for sJ^d_{CDW2} junctions. At the same time, just this behavior is responsible for abnormal deviations of $\boldsymbol{i}_c\{\alpha\}\boldsymbol{\delta}\boldsymbol{\delta}'$ correlations from the law of corresponding states in the case of nJ^d_{CDW2} junctions (see Sect. 3.3).

The reduced current $\boldsymbol{i}_c$ is calculated as a ratio between the quantities I_c and I_c^0 determined in a more rigorous way. Nevertheless, as the estimations above show, with rather a high accuracy, this ratio contains a Δ^2-term in both limiting T-regions and, additionally, a Δ-term at $T \to 0$ (see formulas (A.3) and (A.4)). The latter should be more pronounced at small α to produce a square-root

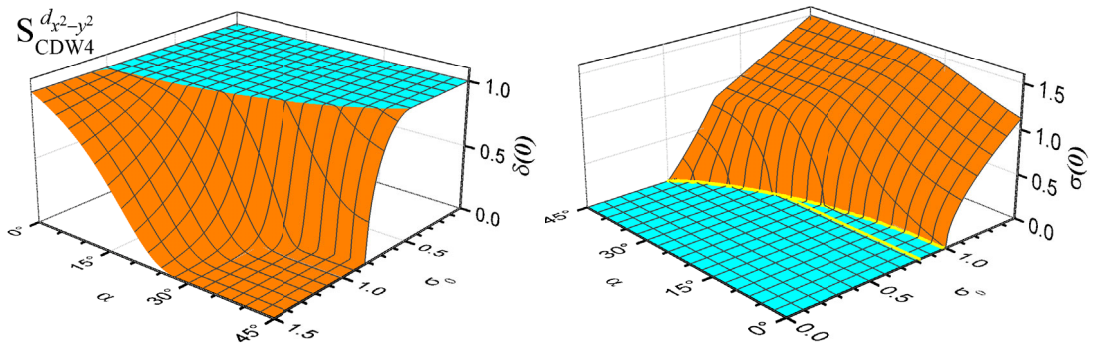

Fig. A.1. Dependences of the actual normalized zero-temperature order parameter values $\delta(0)$ (panel a) and $\sigma(0)$ (panel b) for the S^d_{CDW4} superconductor on the parent problem parameters α and σ_0. In panel (b), the boundaries of the phase diagram area where the reentrance occurs are shown by bright curves.

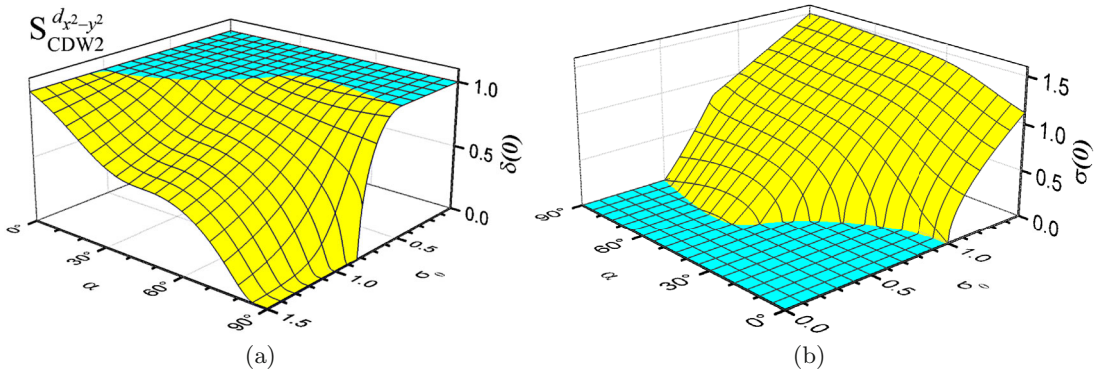

Fig. A.2. The same as in Figure A.1, but for the S^d_{CDW2} superconductor.

singularity at small δ's, e.g., in the $\boldsymbol{i}_c\{\sigma_0\}\boldsymbol{\delta}^2$-dependences. Exactly this behavior is really revealed in our calculations (see the right panel of Fig. 5b as an example). In other cases, the approximate proportionality between $\boldsymbol{i}_c$ and $\boldsymbol{\delta}^2$ holds true in a wider temperature range.

Thus, a simple analysis of formulas (A.3) and (A.4) brings us to a conclusion that it is just the appearance of CDWs that is responsible for the deviations in the $\boldsymbol{i}_c\{x\}\boldsymbol{\delta}^2$-dependences from the law of corresponding states. This conclusion is valid for various physical quantities x that govern the magnitude of superconducting order parameter in partially gapped CDW superconductors, namely, the temperature T, the relative strength of dielectric and superconducting pairing Σ_0/Δ_0, and the degree of FS dielectric gapping α. As a result, those deviations can be used to indirectly detect CDWs in the examined objects.

References

1. J. Bardeen, L.N. Cooper, J.R. Schrieffer, Phys. Rev. **108**, 1175 (1957)
2. V. Ambegaokar, A. Baratoff, Phys. Rev. Lett. **10**, 486 (1963)
3. V. Ambegaokar, A. Baratoff, Phys. Rev. Lett. **11**, 104 (1963)
4. W.A. Harrison, Phys. Rev. **123**, 85 (1961)
5. J. Bardeen, Phys. Rev. Lett. **6**, 57 (1961)
6. M.H. Cohen, L.M. Falicov, J.C. Phillips, Phys. Rev. Lett. **8**, 316 (1962)
7. A.E. Gorbonosov, I.O. Kulik, Fiz. Met. Metalloved. **23**, 803 (1967)
8. A.E. Gorbonosov, I.O. Kulik, Zh. Eksp. Teor. Fiz. **55**, 876 (1968)
9. J.R. Schrieffer, X.G. Wen, S.C. Zhang, Phys. Rev. B **39**, 11663 (1989)
10. T. Moriya, Y. Takahashi, K. Ueda, J. Phys. Soc. Jpn **59**, 2905 (1990)
11. P. Monthoux, A.V. Balatsky, D. Pines, Phys. Rev. Lett. **67**, 3448 (1991)
12. Q. Chen, I. Kosztin, B. Jankó, K. Levin, Phys. Rev. Lett. **81**, 4708 (1998)
13. K. Maki, S. Haas, Phys. Rev. B **67**, 020510 (2003)
14. C. Bruder, A. van Otterlo, G.T. Zimanyi, Phys. Rev. B **51**, 12904 (1995)
15. Yu. S. Barash, A.V. Galaktionov, A.D. Zaikin, Phys. Rev. Lett. **75**, 1676 (1995)
16. P.W. Anderson, in *Lectures on the Many-Body Problem*, edited by E.R. Caianiello (Academic Press, New York, 1964), Vol. 2, p. 113

17. A. Barone, G. Paterno, *The Physics and Applications of the Josephson Effect* (John Wiley and Sons, New York, 1982)
18. B. Mühlschlegel, Z. Phys. **155**, 313 (1959)
19. A.M. Gabovich, A.I. Voitenko, T. Ekino, M.S. Li, H. Szymczak, M. Pękała, Adv. Condens. Matter Phys. **2010**, 681070 (2010)
20. H. Won, K. Maki, Phys. Rev. B **49**, 1397 (1994)
21. H. Won, K. Maki, E. Puchkaryov, in *High-Tc Superconductors and Related Materials. Material Science, Fundamental Properties, and Some Future Electronic Applications*, edited by S.L. Drechsler, T. Mishonov (Kluwer Academic, Dordrecht, 2001), p. 375
22. R. Meservey, B.B. Schwartz, in *Superconductivity*, edited by R.D. Parks (Dekker, New York, 1969), Vol. 1, p. 117
23. A.M. Gabovich, V.I. Kuznetsov, Eur. J. Phys. **34**, 371 (2013)
24. D. Kondepudi, I. Prigogine, *Modern Thermodynamics. From Heat Engines to Dissipative Structures* (John Wiley and Sons, Chichister, 1999)
25. T.N. Antsygina, V.A. Slyusarev, Fiz. Nizk. Temp. **22**, 985 (1996)
26. E.S. Borovik, V.V. Eremenko, A.S. Mil'ner, *Lectures on Magnetism* (Fizmatlit, Moscow, 2005), in Russian
27. D.J. Thouless, Phys. Rev. **117**, 1256 (1960)
28. J.F. Annett, Contemp. Phys. **36**, 423 (1995)
29. V.P. Mineev, K.V. Samokhin, *Introduction to Unconventional Superconductivity* (Gordon and Breach Science Publishers, Amsterdam, 1999)
30. M. Ledvij, R.A. Klemm, Phys. Rev. B **51**, 3269 (1995)
31. J.Y.T. Wei, N.-C. Yeh, D.F. Garrigus, M. Strasik, Phys. Rev. Lett. **81**, 2542 (1998)
32. A.M. Gabovich, A.I. Voitenko, Fiz. Nizk. Temp. **26**, 419 (2000)
33. A.M. Gabovich, A.I. Voitenko, J.F. Annett, M. Ausloos, Supercond. Sci. Technol. **14**, R1 (2001)
34. A.M. Gabovich, A.I. Voitenko, M. Ausloos, Phys. Rep. **367**, 583 (2002)
35. T. Ekino, A.M. Gabovich, M.S. Li, M. Pękała, H. Szymczak, A.I. Voitenko, Symmetry **3**, 699 (2011)
36. T. Ekino, A.M. Gabovich, M.S. Li, M. Pękała, H. Szymczak, A.I. Voitenko, J. Phys.: Condens. Matter **23**, 385701 (2011)
37. T. Yoshida, M. Hashimoto, I.M. Vishik, Z.-X. Shen, A. Fujimori, J. Phys. Soc. Jpn **81**, 011006 (2012)
38. S.E. Sebastian, N. Harrison, G.G. Lonzarich, Rep. Prog. Phys. **75**, 102501 (2012)
39. V.B. Zabolotnyy, A.A. Kordyuk, D. Evtushinsky, V.N. Strocov, L. Patthey, T. Schmitt, D. Haug, C.T. Lin, V. Hinkov, B. Keimer, B. Büchner, S.V. Borisenko, Phys. Rev. B **85**, 064507 (2012)
40. G. Coslovich, C. Giannetti, F. Cilento, S. Dal Conte, T. Abebaw, D. Bossini, G. Ferrini, H. Eisaki, M. Greven, A. Damascelli, F. Parmigiani, Phys. Rev. Lett. **110**, 107003 (2013)
41. A.M. Gabovich, A.I. Voitenko, Fiz. Nizk. Temp. **39**, 301 (2013)
42. B. Vignolle, D. Vignolles, M.-H. Julien, C. Proust, C.R. Physique **14**, 39 (2013)
43. A.I. D'yachenko, V.Yu. Tarenkov, S.L. Sidorov, V.N. Varyukhin, A.L. Solovjov, Fiz. Nizk. Temp. **39**, 416 (2013)
44. P. Hosur, A. Kapitulnik, S.A. Kivelson, J. Orenstein, S. Raghu, Phys. Rev. B **87**, 115116 (2013)
45. E. Uykur, K. Tanaka, T. Masui, S. Miyasaka, S. Tajima, J. Phys. Soc. Jpn **82**, 033701 (2013)
46. S. Hüfner, F. Müller, Physica C **485**, 83 (2013)
47. J.W. Alldredge, K. Fujita, H. Eisaki, S. Uchida, K. McElroy, Phys. Rev. B **87**, 104520 (2013)
48. G. Ghiringhelli, M. Le Tacon, M.M.S. Blanco-Canosa, C. Mazzoli, N.B. Brookes, G.M. De Luca, A. Frano, D.G. Hawthorn, F. He, T. Loew, M.M. Sala, D.C. Peets, M. Salluzzo, E. Schierle, R. Sutarto, G.A. Sawatzky, E. Weschke, B. Keimer, L. Braicovich, Science **337**, 821 (2012)
49. E. Blackburn, J. Chang, M. Hücker, A.T. Holmes, N.B. Christensen, R. Liang, D.A. Bonn, W.N. Hardy, U. Rütt, O. Gutowski, M. von Zimmermann, E.M. Forgan, S.M. Hayden, Phys. Rev. Lett. **110**, 137004 (2013)
50. J. Fink, E. Schierle, E. Weschke, J. Geck, Rep. Prog. Phys. **76**, 056502 (2013)
51. S.-H. Baek, P.C. Hammel, M. Hücker, B. Büchner, U. Ammerahl, A. Revcolevschi, B.J. Suh, Phys. Rev. B **87**, 174505 (2013)
52. A. Shekhter, B.J. Ramshaw, R. Liang, W.N. Hardy, D.A. Bonn, F.F. Balakirev, R.D. McDonald, J.B. Betts, S.C. Riggs, A. Migliori, Nature **498**, 75 (2013)
53. J.A. Rosen, R. Comin, G. Levy, D. Fournier, Z.-H. Zhu, B. Ludbrook, C.N. Veenstra, A. Nicolaou, D. Wong, P. Dosanjh, Y. Yoshida, H. Eisaki, G.R. Blake, F. White, T.T.M. Palstra, R. Sutarto, F. He, A.F. Pereira, Y. Lu, B. Keimer, G. Sawatzky, L. Petaccia, A. Damascelli, Nat. Commun. **4**, 1977 (2013)
54. T. Wu, H. Mayaffre, S. Krämer, M. Horvatić, C. Berthier, P.L. Kuhns, A.P. Reyes, R. Liang, W.N. Hardy, D.A. Bonn, M.-H. Julien, Nat. Commun. **4**, 2113 (2013)
55. T. Wu, H. Mayaffre, S. Krämer, M. Horvatić, C. Berthier, C.T. Lin, D. Haug, T. Loew, V. Hinkov, B. Keimer, M.-H. Julien, Phys. Rev. B **88**, 014511 (2013)
56. D.G. Hawthorn, K.M. Shen, J. Geck, D.C. Peets, H. Wadati, J. Okamoto, S.-W. Huang, D.J. Huang, H.-J. Lin, J.D. Denlinger, R. Liang, D.A. Bonn, W.N. Hardy, G.A. Sawatzky, Phys. Rev. B **84**, 075125 (2011)
57. S. Blanco-Canosa, A. Frano, T. Loew, Y. Lu, J. Porras, G. Ghiringhelli, M. Minola, C. Mazzoli, L. Braicovich, E. Schierle, E. Weschke, M. Le Tacon, B. Keimer, Phys. Rev. Lett. **110**, 187001 (2013)
58. V. Thampy, S. Blanco-Canosa, M. García-Fernández, M.P.M. Dean, G.D. Gu, M. Först, T. Loew, B. Keimer, M. Le Tacon, S.B. Wilkins, J.P. Hill, Phys. Rev. B **88**, 024505 (2013)
59. P.A. Lee, T.M. Rice, P.W. Anderson, Phys. Rev. Lett. **31**, 462 (1973)
60. M.V. Sadovskii, Usp. Fiz. Nauk **171**, 539 (2001)
61. N. Doiron-Leyraud, S. Lepault, O. Cyr-Choinière, B. Vignolle, G. Grissonnanche, F. Laliberté, J. Chang, N. Barišić, M.K. Chan, L. Ji, X. Zhao, Y. Li, M. Greven, C. Proust, L. Taillefer, Phys. Rev. X **3**, 021019 (2013)
62. C.C. Tsuei, J.R. Kirtley, Rev. Mod. Phys. **72**, 969 (2000)
63. J.R. Kirtley, C.R. Physique **12**, 436 (2011)
64. R.A. Klemm, Philos. Mag. **85**, 801 (2005)
65. G.-M. Zhao, Phys. Scr. **83**, 038302 (2011)
66. A.M. Gabovich, M.S. Li, H. Szymczak, A.I. Voitenko, Phys. Rev. B **87**, 104503 (2013)

67. A.M. Gabovich, A.I. Voitenko, Phys. Rev. B **80**, 224501 (2009)
68. A.I. Voitenko, A.M. Gabovich, Fiz. Nizk. Temp. **36**, 1300 (2010)
69. A.I. Voitenko, A.M. Gabovich, Fiz. Tverd. Tela **52**, 20 (2010)
70. A.M. Gabovich, M.S. Li, H. Szymczak, A.I. Voitenko, in *Superconductors – Materials, Properties and Applications*, edited by A. Gabovich (InTech, Rijeka, Croatia, 2012), p. 289
71. A.M. Gabovich, A.I. Voitenko, Fiz. Nizk. Temp. **38**, 414 (2012)
72. G. Bilbro, W.L. McMillan, Phys. Rev. B **14**, 1887 (1976)
73. C.A. Balseiro, L.M. Falicov, Phys. Rev. B **20**, 4457 (1979)
74. A.M. Gabovich, E.A. Pashitskii, A.S. Shpigel, Zh. Eksp. Teor. Fiz. **77**, 1157 (1979)
75. A.M. Gabovich, D.P. Moiseev, A.S. Shpigel, J. Phys. C **15**, L569 (1982)
76. A.M. Gabovich, A.S. Shpigel, J. Low Temp. Phys. **51**, 581 (1983)
77. A.M. Gabovich, A.S. Gerber, A.S. Shpigel, Phys. Stat. Sol. B **141**, 575 (1987)
78. A.M. Gabovich, A.S. Shpigel, Phys. Rev. B **38**, 297 (1988)
79. A.M. Gabovich, D.P. Moiseev, A.S. Shpigel, A.I. Voitenko, Phys. Stat. Sol. B **161**, 293 (1990)
80. A.M. Gabovich, Fiz. Nizk. Temp. **18**, 693 (1992)
81. A.M. Gabovich, A.I. Voitenko, Europhys. Lett. **38**, 371 (1997)
82. A.M. Gabovich, A.I. Voitenko, Phys. Rev. B **55**, 1081 (1997)
83. A.M. Gabovich, M.S. Li, H. Szymczak, A.I. Voitenko, J. Phys.: Condens. Matter **15**, 2745 (2003)
84. T. Ekino, A.M. Gabovich, A.I. Voitenko, Fiz. Nizk. Temp. **31**, 77 (2005)
85. T. Ekino, A.M. Gabovich, M.S. Li, M. Pękała, H. Szymczak, A.I. Voitenko, Jpn J. Appl. Phys. **45**, 2242 (2006)
86. A.M. Gabovich, A.I. Voitenko, Phys. Rev. B **75**, 064516 (2007)
87. T. Ekino, A.M. Gabovich, A.I. Voitenko, Fiz. Nizk. Temp. **34**, 515 (2008)
88. T. Ekino, A.M. Gabovich, M.S. Li, M. Pękała, H. Szymczak, A.I. Voitenko, J. Phys.: Condens. Matter **20**, 425218 (2008)
89. W. Haberkorn, H. Knauer, J. Richter, Phys. Stat. Sol. A **47**, K161 (1978)
90. A.A. Golubov, M.Yu. Kupriyanov, E. Il'ichev, Rev. Mod. Phys. **76**, 411 (2004)
91. R.S. Markiewicz, J. Phys. Chem. Sol. **58**, 1179 (1997)
92. N.M. Plakida, *High-Temperature Cuprate Superconductors. Experiment, Theory, and Applications* (Springer-Verlag, Berlin, 2010)
93. P. Abbamonte, A. Rusydi, S. Smadici, G.D. Gu, G.A. Sawatzky, D.L. Feng, Nat. Phys. **1**, 155 (2005)
94. M. Fujita, H. Hiraka, M. Matsuda, M. Matsuura, J.M. Tranquada, S. Wakimoto, G. Xu, K. Yamada, J. Phys. Soc. Jpn **81**, 011007 (2012)
95. T. Das, Phys. Rev. B **87**, 144505 (2013)
96. S.A. Kivelson, I.P. Bindloss, E. Fradkin, V. Oganesyan, J.M. Tranquada, A. Kapitulnik, C. Howald, Rev. Mod. Phys. **75**, 1201 (2003)
97. S. Sugai, Y. Takayanagi, N. Hayamizu, Phys. Rev. Lett. **96**, 137003 (2006)
98. D.H. Torchinsky, F. Mahmood, A.T. Bollinger, I. Božović, N. Gedik, Nat. Mater. **12**, 387 (2013)
99. J.L. Tallon, F. Barber, J.G. Storey, J.W. Loram, Phys. Rev. B **87**, 140508 (2013)
100. S. Yoshizawa, T. Koseki, K. Matsuba, T. Mochiku, K. Hirata, N. Nishida, J. Phys. Soc. Jpn **82**, 083706 (2013)
101. M. Vojta, Adv. Phys. **58**, 699 (2009)
102. E. Fradkin, S.A. Kivelson, M.J. Lawler, J.P. Eisenstein, A.P. Mackenzie, Annu. Rev. Condens. Matter Phys. **1**, 153 (2010)
103. S.I. Mirzaei, D. Stricker, J.N. Hancock, C. Berthod, A. Georges, E. van Heumen, M.K. Chan, X. Zhao, Y. Li, M. Greven, N. Barišić, D. van der Marel, Proc. Natl. Acad. Sci. USA **110**, 5774 (2013)
104. A.I. Posazhennikova, M.V. Sadovskii, Zh. Eksp. Teor. Fiz. **115**, 632 (1999)
105. J. Schmalian, D. Pines, B. Stojković, Phys. Rev. B **60**, 667 (1999)
106. I.O. Kulik, I.K. Yanson, *Josephson Effect in Superconducting Tunnel Structures* (Israel Program for Scientific Translation, Jerusalem, 1972)
107. F. Tafuri, J.R. Kirtley, Rep. Prog. Phys. **68**, 2573 (2005)
108. Yu.S. Barash, A.V. Galaktionov, A.D. Zaikin, Phys. Rev. B **52**, 665 (1995)
109. Yu.S. Barash, H. Burkhardt, D. Rainer, Phys. Rev. Lett. **77**, 4070 (1996)
110. Y.-M. Nie, L. Coffey, Phys. Rev. B **59**, 11982 (1999)
111. Y. Tanaka, Phys. Rev. Lett. **72**, 3871 (1994)
112. J.H. Xu, J.L. Shen, J.H. Miller Jr., C.S. Ting, Phys. Rev. Lett. **73**, 2492 (1994)
113. J.H. Xu, J.L. Shen, J.H. Miller Jr., C.S. Ting, Phys. Rev. Lett. **75**, 1677 (1995)
114. Yu.S. Barash, A.A. Svidzinskii, Zh. Eksp. Teor. Fiz. **111**, 1120 (1997)
115. S. Kashiwaya, Y. Tanaka, Rep. Prog. Phys. **63**, 1641 (2000)
116. K. Kouznetsov, L. Coffey, Phys. Rev. B **54**, 3617 (1996)
117. Y.-M. Nie, L. Coffey, Phys. Rev. B **57**, 3116 (1998)
118. Yu.M. Shukrinov, A. Namiranian, A. Najafi, Fiz. Nizk. Temp. **27**, 15 (2001)
119. A. Sharoni, G. Leibovitch, A. Kohen, R. Beck, G. Deutscher, G. Koren, O. Millo, Europhys. Lett. **62**, 883 (2003)
120. B.D. Josephson, Phys. Lett. **1**, 251 (1962)
121. T. Löfwander, V.S. Shumeiko, G. Wendin, Supercond. Sci. Technol. **14**, R53 (2001)
122. J.F. Annett, N.D. Goldenfeld, A.J. Leggett, in *Physical Properties of High Temperature Superconductors V*, edited by D.M. Ginsberg (World Scientific, River Ridge, NJ, 1996), p. 375–461
123. C.C. Tsuei, J.R. Kirtley, in *Superconductivity. Novel Superconductors*, edited by K.H. Bennemann, J.B. Ketterson (Springer-Verlag, Berlin, 2008), Vol. 2, p. 869
124. I.O. Kulik, A.N. Omelyanchuk, Pis'ma Zh. Eksp. Teor. Fiz. **21**, 216 (1975)
125. I.O. Kulik, A.N. Omel'yanchuk, Fiz. Nizk. Temp. **3**, 945 (1977)
126. I.O. Kulik, A.N. Omel'yanchuk, Fiz. Nizk. Temp. **4**, 296 (1978)
127. A.F. Andreev, Zh. Eksp. Teor. Fiz. **46**, 1823 (1964)
128. D. Saint-James, J. Phys. (Paris) **25**, 899 (1964)
129. G.E. Blonder, M. Tinkham, T.M. Klapwijk, Phys. Rev. B **25**, 4515 (1982)

130. P.A.M. Benistant, A.P. van Gelder, H. van Kempen, P. Wyder, Phys. Rev. B **32**, 3351 (1985)
131. G. Deutscher, Rev. Mod. Phys. **77**, 109 (2005)
132. D. Daghero, M. Tortello, P. Pecchio, V.A. Stepanov, R.S. Gonnelli, Fiz. Nizk. Temp. **39**, 261 (2013)
133. M. Sigrist, T.M. Rice, J. Phys. Soc. Jpn **61**, 4283 (1992)
134. Yu.S. Barash, Phys. Rev. B **61**, 678 (2000)
135. S. Shirai, H. Tsuchiura, Y. Tanaka, J. Inoue, S. Kashiwaya, J. Low Temp. Phys. **131**, 503 (2003)
136. S. Ueda, T. Yamaguchi, Y. Kubo, S. Tsuda, Y. Takano, J. Shimoyama, K. Kishio, J. Appl. Phys. **106**, 074516 (2009)
137. N. Mros, V.M. Krasnov, A. Yurgens, D. Winkler, T. Claeson, Phys. Rev. B **57**, 8135 (1998)
138. T. Kawae, M. Nagao, Y. Takano, H. Wang, T. Hatano, S.-J. Kim, T. Yamashita, Supercond. Sci. Technol. **18**, 1159 (2005)
139. E. Il'ichev, M. Grajcar, R. Hlubina, R.P.J. IJsselsteijn, H.E. Hoenig, H.-G. Meyer, A. Golubov, M.H.S. Amin, A.M. Zagoskin, A.N. Omelyanchouk, M.Yu. Kupriyanov, Phys. Rev. Lett. **86**, 5369 (2001)
140. G. Testa, E. Sarnelli, A. Monaco, E. Esposito, M. Ejrnaes, D.-J. Kang, S.H. Mennema, E.J. Tarte, M.G. Blamire, Phys. Rev. B **71**, 134520 (2005)
141. E.E. Mitchell, J.C. Macfarlane, C.P. Foley, Supercond. Sci. Technol. **24**, 055004 (2011)
142. H. Arie, K. Yasuda, H. Kobayashi, I. Iguchi, Y. Tanaka, S. Kashiwaya, Phys. Rev. B **62**, 11864 (2000)
143. *Tunneling Phenomena in Solids*, edited by E. Burstein, S. Lundqvist (Plenum Press, New York, 1969)
144. A.M. Gabovich, V.A. Medvedev, D.P. Moiseev, A.A. Motuz, A.F. Prikhot'ko, L.V. Prokopovich, A.V. Solodukhin, L.I. Khirunenko, V.K. Shinkarenko, A.S. Shpigel, V.E. Yachmenev, Fiz. Nizk. Temp. **13**, 844 (1987)
145. A.M. Gabovich, A.I. Voitenko, J. Phys.: Condens. Matter **9**, 3901 (1997)
146. H.J.H. Smilde, A.A. Golubov, Ariando, G. Rijnders, J.M. Dekkers, S. Harkema, D.H.A. Blank, H. Rogalla, H. Hilgenkamp, Phys. Rev. Lett. **95**, 257001 (2005)
147. J.R. Kirtley, C.C. Tsuei, A. Ariando, C.J.M. Verwijs, S. Harkema, H. Hilgenkamp, Nat. Phys. **2**, 190 (2006)
148. A. Damascelli, Z. Hussain, Z.-X. Shen, Rev. Mod. Phys. **75**, 473 (2003)
149. A. Sacuto, Y. Gallais, M. Cazayous, M.-A. Méasson, G.D. Gu, D. Colson, Rep. Prog. Phys. **76**, 022502 (2013)
150. Z.G. Ivanov, E.A. Stepantsov, T. Claeson, F. Wenger, S.Y. Lin, N. Khare, P. Chaudhari, Phys. Rev. B **57**, 602 (1998)
151. H. Hilgenkamp, Supercond. Sci. Technol. **21**, 034011 (2008)
152. F. Tafuri, D. Massarotti, L. Galletti, D. Stornaiuolo, D. Montemurro, L. Longobardi, P. Lucignano, G. Rotoli, G.P. Pepe, A. Tagliacozzo, F. Lombardi, J. Supercond. **26**, 21 (2013)